DELIVERABLE 4.1.1[1]

CONTRACT N°	**SPC8-GA-2009-233655**	
PROJECT N°	**FP7-233655**	
ACRONYM	**CITYHUSH**	
TITLE	**Acoustically green road vehicles and city areas**	
Work Package 4	**Propagation attenuation of road traffic noise**	
4.1	Wave propagation analysis for heavy quiet vehicle tyres	
Written by	**University of Cambridge**	
Due submission date	**31.12.2011**	
Actual submission date	**23.02.2012**	
Project Co-Ordinator	Acoustic Control	ACL SE
Partners	Accon	ACC DE
	Alfa Products & Technologies	APT BE
	Goodyear	GOOD LU
	Head Acoustics	HAC DE
	Royal Institute of Technology	KTH SE
	NCC Roads	NCC SE
	Stockholm Environmental & Health Administration	SEP SE
	Netherlands Organisation for Applied Scientific Research	TNO NL
	Trafikkontoret Göteborg	TRAF SE
	TT&E Consultants	TTE GR
	University of Cambridge	UCAM UK
	Promation of Operational Links with Integrated Services	POLIS BE
Project start date	**January 1, 2010**	
Duration of the project	**36 months**	

Project funded by the European Commission within the Seventh Framework program

Dissemination Level

PU	Public	✓
PP	Restricted to other programme participants (including the Commission Services)	
RE	Restrictec to a group specified by the consortium (including the Commission Services)	
CO	Confidential, only for the members of the consortium (including the Commission Services)	

Nature of Deliverable

R	Report	✓
P	Prototype	
D	Demonstrator	
C	Other	

SEVENTH FRAMEWORK PROGRAMME

TABLE OF CONTENTS

0 Executive summary 3
0.1 Objective of the deliverable 3
0.2 Description of the work performed since the beginning of the project 3
0.3 Main results achieved so far 3
0.4 Expected final results 3
0.5 Potential impact and use 3
0.6 Partners involved and their contribution 3
0.7 Conclusions 3
1 Background 4
1.1 NOISE SOURCES 4
1.1.1 Power unit 4
1.1.2 Tyre/road 4
1.1.3 Wind oscillation 4
1.2 THE DIFFERENCE BETWEEN HEAVY AND LIGHT VEHICLES 4
1.2.1 Source distribution of heavy vehicles 4
1.2.2 Discussion 5
1.3 The horn effect 6
1.4 Horn effect characteristics 6
1.5 Objectives 7
1.6 Content 7
2 Theoretical considerations 8
2.1 Horn amplification 8
2.2 Reciprocity 8
2.3 Scaling considerations and the far-field form 9
3 Numerical methodology 10
3.1 The boundary element code 10
3.2 Geometry specification and mesh generation 10
3.3 Ground-plane representation 12
3.4 Mesh resolution 12
4 Results 15
4.1 Test cases 15
4.2 Reference case 15
4.3 Effect of width 18
4.4 Effect of crown radius 21
5 Discussion 26
5.1 Sharp-shouldered geometries 26
5.2 Crown radius recommendations 28
6 Conclusions 31
References 32
APPENDIX 33

0 EXECUTIVE SUMMARY

0.1 OBJECTIVE OF THE DELIVERABLE

To provide recommendations for optimal tyre dimensions for heavy vehicles, on the basis of the radiative characteristics of the tyre geometry.

0.2 DESCRIPTION OF THE WORK PERFORMED SINCE THE BEGINNING OF THE PROJECT

A reciprocal-configuration Boundary Element Method calculation of acoustic radiation characteristics has been implemented for a generic tyre geometry. The influence of the geometric parameters on the radiation characteristics has been studied. Based on the results, recommendations for acoustically optimal truck tyre dimensions have been formulated.

0.3 MAIN RESULTS ACHIEVED SO FAR

The degree of amplification of noise sources on the tyre belt is strongly affected by the overall tyre width. In contrast, the tyre radius predominantly influences the pattern of the varying amplification around the belt, rather than its absolute level. Radiusing the tyre's 'shoulder' region is potentially beneficial in terms of lowering amplification levels, for a tyre of fixed overall width. However, it is less effective than maintaining sharp shoulders and reducing the overall width.

0.4 EXPECTED FINAL RESULTS

As Section 0.3.

0.5 POTENTIAL IMPACT AND USE

The recommendations developed here give straightforward guidelines for engineers wishing to design quiet tyres for heavy vehicles, and for road vehicles in general.

0.6 PARTNERS INVOLVED AND THEIR CONTRIBUTION

The main work described in this report was performed by UCAM. The background for tyre/road noise from heavy traffic was performed by ACL.

0.7 CONCLUSIONS

For an acoustically optimal belted tyre, the overall width should be as small as possible, even if this leads to a larger diameter. The width should not be increased in order to accommodate a radiused crown region.

1 BACKGROUND

1.1 NOISE SOURCES

1.1.1 Power unit

The powertrain consists of components generating the power of the vehicle. This component consists of the combustion engine, transmission, drive shafts, exhaust and differentials of the engine. This is source that is most commonly falsely referred to as the main noise source of all vehicles. The level of noise is determined by the engine load and the rotational speed of the engine ro. Noise from the power unit consists of several sub-sources where the engine, exhaust, fans and intake systems is the major sources. The power unit generates most kind of noise, transient

1.1.2 Tyre/road

Noise generated in this source group is defined to the noise generated by rolling of the tyres on a surface. The noise defining aspects of this source group is the speed of the vehicle, the material and tread pattern of the tyre, the texture and material of the road but also highly dependent of the load of the tyres that exists during acceleration and braking.

1.1.3 Wind oscillation

Noise generated in the source group is aerodynamic source and related to the turbulent airflow generated by the vehicles speed, external components and the shaping of the vehicle chassis. Aerodynamic noise is generated at higher speed, over 110 km/h and is more important to the interior noise level of the vehicle then the exterior noise.

1.2 THE DIFFERENCE BETWEEN HEAVY AND LIGHT VEHICLES

Vehicle has beendivided into two categories because of the large variety of vehicles in our contemporary society. The noise source distribution depends of several attributes such as size of the vehicle, total weight, engine power etc.

1.2.1 Source distribution of heavy vehicles

Heavier vehicles attributes such as larger frame, more powerful engine, heavier weight influences the noise source distribution greatly. Figure 1.1, displays the contribution of the different noise sources at different velocities. At lower speeds it's the propulsion noise generated by the power unit that is the most dominant noise source at lower

velocities. The rolling noises contribution generated by the tyre-road interaction starts to add its contribution to the total noise level at roughly 20 km/h and is the dominant noise source at roughly 75 km/h.

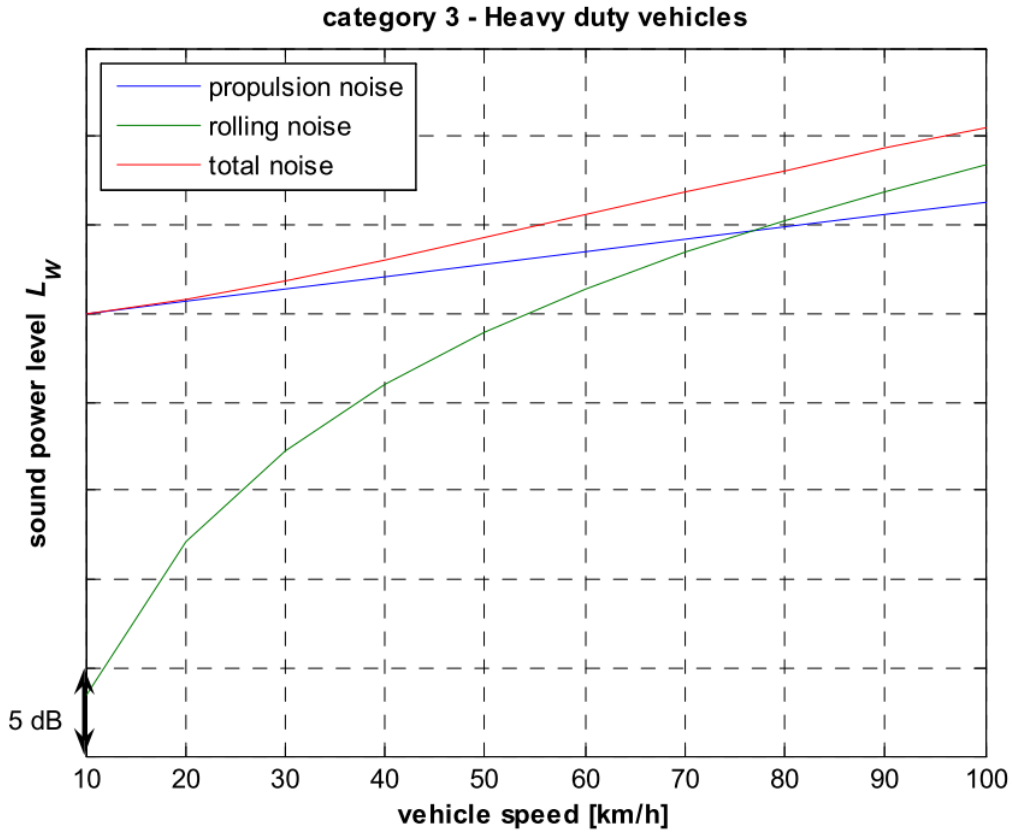

Figure 1.1 At lower speed of 0-75 km/h the powertrain of the vehicle is the predominant source of noise. At vehicle speeds above 75 km/h the predominant source of noise for vehicles is the interaction between the vehicles tire and the surface of the road.

1.2.2 Discussion

Because of the low speed limits in contemporary urban environment the effect of a quieter tyre for heavier vehicles can be discussed. The main noise generation source at lower speeds is the power unit. Noise generated by the tyre-road interaction starts to become a dominant sound source at roughly 75 km/h, a velocity that rarely occurs in European cities. Although at 20 km/h the tyre noise starts to add its contribution to total noise level generated by the vehicle. And at 30 to 50 km/h, normal occurring speeds in most cities the tyre noise generation contributes with an added 1 to 2 dB to the total noise level.

Although quieter tyres could make larger difference in the noise radiation if transit routes with higher velocities and larger portions of heavier transports are taken into consideration. A traffic solution present in most European cities.

1.3 THE HORN EFFECT

The 'horn effect' is the name given to the selective amplification of tyre vibration sources on the belt in the region of the contact patch. It is so called because of the horn-like geometry formed by the tyre belt and the road surface, and (depending on the frequency and geometrical factors) can be highly significant, increasing sound levels by a factor of over 20dB relative to those due to the same source in the absence of the tyre.

1.4 HORN EFFECT CHARACTERISTICS

A thorough investigation of the horn effect was carried out, in two parts, by Graf, Kuo and co-workers [1,2]. The base geometry was typical of a passenger car tyre, with diameter 64cm and width 20cm. At very low frequencies, below 100Hz, effectively no amplification was found. A significant horn effect was only observed once the acoustic wavelength was reduced below the tyre diameter, increasing typically (for a listener in front of the tyre) to in excess of 20dB. The frequency at which the maximum amplification occurs was found to vary, depending on the proximity of the source to the contact patch edge. However, very close to this edge, the behaviour becomes independent of source location, and the frequency range for high amplification is extensive (from around 2 to 4kHz). At higher frequencies, interference effects lead to a lobed amplification pattern.

The directivity of the horn effect was also investigated. At the low frequencies, the amplification is associated with a dipole whose strength is the overall force exerted by the source on the tyre, and this is reflected in the directivity pattern. Once the tyre is no longer compact, more lobes develop, and the dependence on the locations of source and receiver becomes greater.

Graf et al did not fully probe the influence of tyre geometry on the horn effect. However, they did show a significant impact of belt width on the amplification at lower frequencies, and (for relatively distant sources) a tendency for edge rounding to reduce the amplification slightly. Further work on this topic was carried out by O'Boy [3], in the course of the QCITY project. For a tyre of the same diameter, and width 18cm, O'Boy found that belt edges with radius 3cm had little effect, but that a 3dB reduction was obtainable with further rounding to 6cm. The generalisation of these results to tyres of significantly different diameter was not addressed. In particular, the question of optimal truck tyre geometry for reduced horn amplification remains open.

1.5 OBJECTIVES

The fundamental objective of the current work is to investigate geometrical influences on the horn effect for tyre sizes typical of heavy vehicles, and thereby to produce recommendations for quiet designs. However, rather than restrict the study to this size range in particular, it is more productive to take an approach which allows generalisation across a range of sizes. A secondary objective is therefore to develop a methodology which enables this approach.

1.6 CONTENT

The remainder of this report consists of four main parts. In Section 2, the theoretical background for the horn effect evaluation is set out. Section 3 describes the numerical approach taken, and its implementation. The results of the calculations are then presented in Section 4. Finally, Section 5 discusses the implications for truck tyre geometry optimisation.

2 THEORETICAL CONSIDERATIONS

2.1 HORN AMPLIFICATION

As noted above, the horn amplification is quantified with reference to a notional configuration with the tyre absent. This is shown schematically in Figure 2.1. Figure 2.1(a) shows the tyre and ground plane, with a source at (vector) position $\mathbf{x} = \mathbf{x}_s$ and a receiver at $\mathbf{x} = \mathbf{x}_r$. The configuration with the tyre absent is shown in Figure 2.1(b). Note that the source and receiver locations are unchanged, and that the ground plane is still present.

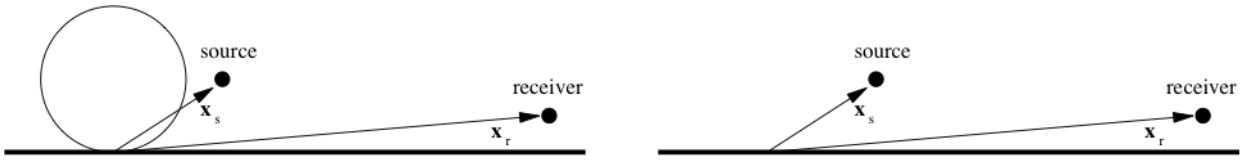

Figure 2.1 Acoustic configurations for horn amplification definition: (a) with tyre; (b) without tyre.

The acoustic pressure at the receiver with the tyre in position is denoted as $p(\mathbf{x}_r, \mathbf{x}_s, t)$, and its counterpart with the tyre absent as $p_{ref}(\mathbf{x}_r, \mathbf{x}_s, t)$. A time-harmonic variation, i.e. $p(\mathbf{x}_r, \mathbf{x}_s, t) = P(\mathbf{x}_r, \mathbf{x}_s, \omega)e^{i\omega t}$, is assumed. The horn amplification is then defined as:

$$H(\mathbf{x}_r, \mathbf{x}_s, \omega) = \frac{P(\mathbf{x}_r, \mathbf{x}_s, \omega)}{P_{ref}(\mathbf{x}_r, \mathbf{x}_s, \omega)}. \tag{2.1}$$

Note that the source strength does not enter this definition. It is implicitly assumed that the source is the same in both configurations, so the amplification is independent of its strength.

The definition of horn amplification presented here allows the source, in principle, to be anywhere in the acoustic space. In practice, it is located on the tyre belt, and this restriction will be assumed from here on.

2.2 RECIPROCITY

The equations of acoustics admit a reciprocal theorem; a particularly useful version of it is stated by Pierce as: 'the ratio of pressure amplitude to source strength remains the same if locations of source and listener and interchanged' [4]. In the notation introduced above, this implies that

$$P(\mathbf{x}_r, \mathbf{x}_s, \omega) = P(\mathbf{x}_s, \mathbf{x}_r, \omega). \tag{2.2}$$

The significance of this result in the context of the numerical analysis carried out in this work will be discussed in Section 4.1. Note, however, that it also applies to the reference pressure from the tyre-absent configuration.

2.3 SCALING CONSIDERATIONS AND THE FAR-FIELD FORM

The natural starting point for a generalisation of the horn effect, applicable across a range of tyre sizes, is a non-dimensionalisation based on the tyre radius, R. The frequency is replaced by the dimensionless variable kR, where the acoustic wavenumber k is equal to the radian frequency divided by the sound speed. The tyre geometry is then described in terms of the ratios of its other dimensions to R.

This approach meets a problem once receiver positions have to be specified. The coordinates of these positions must also be non-dimensionalised on R, which implies that a calculation for a given kR is not universal. (Imagine that it is to be used to deduce the horn effect for a tyre twice the size at half the frequency. The parameter kR is unchanged, but the sources have moved in the physical space, to twice their original distance.) The problem can be circumvented by considering receivers in the far field. In this case, for receivers in the vicinity of the ground plane, the height is clearly irrelevant (since the elevation angle tends to zero). Less evidently, so is the receiver distance.

The latter point is most easily proved by considering the reciprocal problem, with the source in the far-field position. The acoustic disturbance incident on the tyre is then a plane wave, moving parallel to the ground plane. The only influence of source distance is on the amplitude of the plane wave, but the horn amplification definition (2.1) is independent of amplitude. The horn amplification thus depends on the source angle only, which is both dimensionless and unaffected by changes in the tyre size.

3 NUMERICAL METHODOLOGY

3.1 THE BOUNDARY ELEMENT CODE

The Boundary Element Method (BEM) is well established as the numerical approach of choice in the solution of exterior acoustics problems. Its chief advantage over the Finite Element Method (FEM) is that only the surfaces of bodies in the domain need be discretised. Although the resulting matrices are full (rather than sparse, as in the FEM), the avoidance of meshing a domain which extends to infinity is invaluable.

The BEM code employed here is OpenBEM, an open-source implementation of the direct BEM with the CHIEF-point extension for the suppression of spurious body resonances [5]. OpenBEM is written for the Matlab programming environment. No mesh-generation utilities are included in the distribution; bespoke routines were written to create the meshes for the current work.

A well-posed exterior acoustics problem is one in which either the pressure or, more commonly, the normal velocity is known on the surfaces of all the bodies in the domain. In the latter case, the first step is to calculate the surface pressures; field pressures are then available via a post-processing analysis. However, for the reciprocal formulation of the horn effect problem, only the first step is required. By the reciprocal theorem, the pressures on the tyre surface due to an exterior source, at $\mathbf{x} = \mathbf{x}_r$, are the same as the pressures at $\mathbf{x} = \mathbf{x}_r$ due to the respective sources on the tyre. Since one is typically concerned with only a few receiver locations, but needs the contribution to the sound at these locations from all points on the belt, the reciprocal formulation is ideal, and is therefore employed here.

3.2 GEOMETRY SPECIFICATION AND MESH GENERATION

The tyre is taken to be cylindrical, with the cross-sectional geometry shown in Figure 3.1: radius R, overall width w, and crown radius R_c. The ratio of width to radius has a maximum allowed value of 1; with this limitation, the maximum crown radius is always set by the overall width, at w/2.

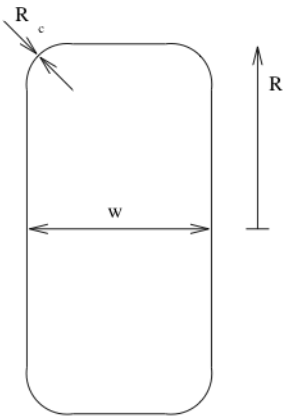

Figure 3.1 Tyre cross-sectional geometry.

The coordinate system for the analysis is shown in Figure 3.2. The z axis is normal to the ground plane, pointing upwards, and the y axis is in the wheel axle direction. The angle θ describes azimuthal locations around the belt. Source locations are characterised by the angle ϕ.

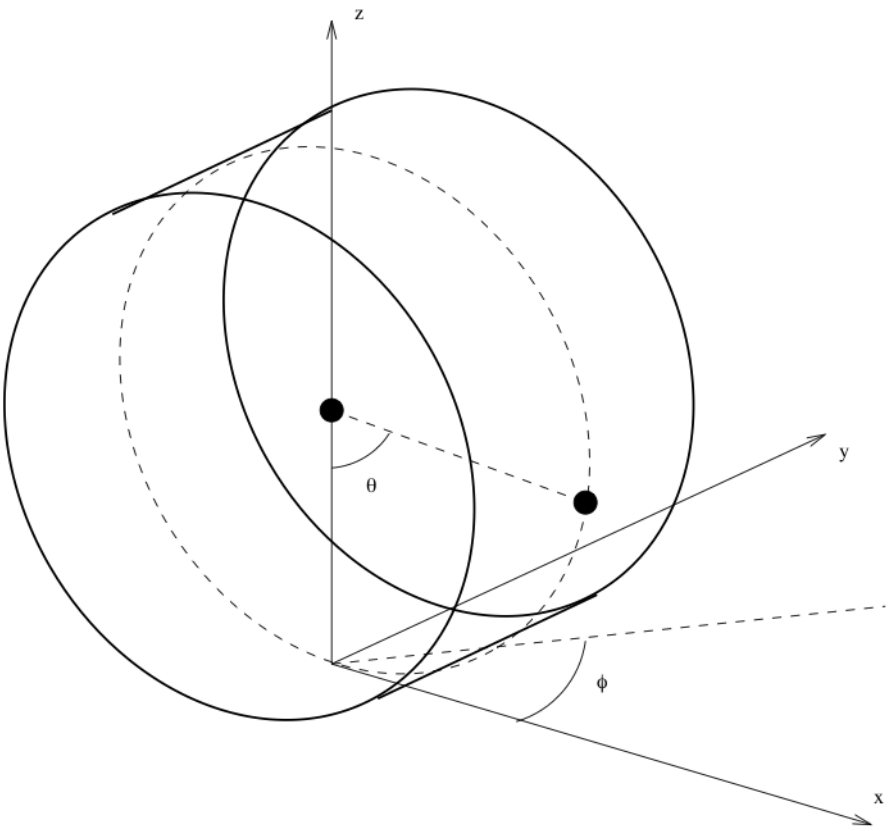

Figure 3.2 Axis system and angular coordinates.

The mesh is arranged in rings, concentric on the sides and parallel on the belt. The number of rings is set by a scale parameter, Δ. In particular, there are $(R–R_c)/\Delta$ (rounded to the nearest integer) rings on each side, $\pi R_c/2\Delta$ in the crown region, and $(w–2R_c)/\Delta$ on the belt. Each ring is filled with triangular elements, starting from six in the first side ring and then increasing with radius. The number of elements in each crown and belt ring is the same. A sample mesh is shown in Figure 3.3.

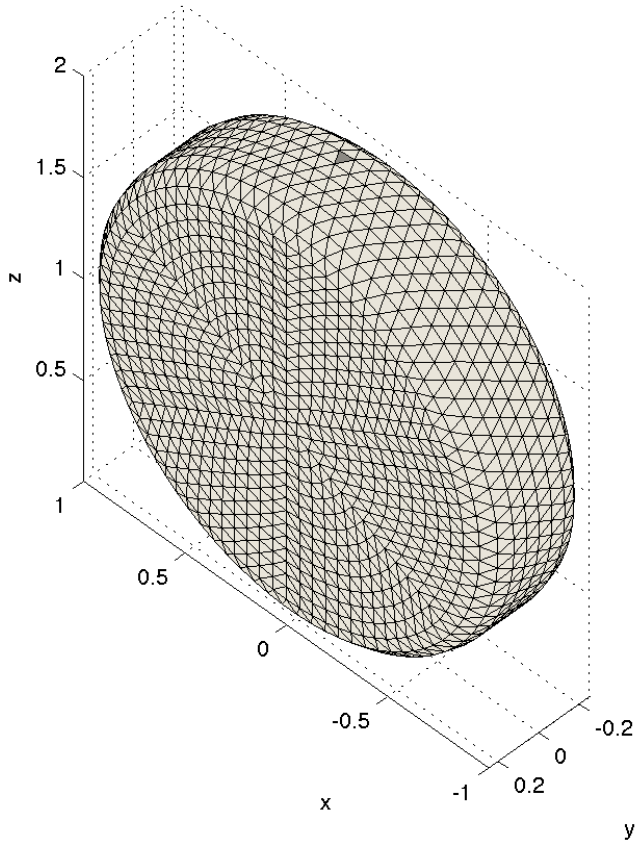

Figure 3.3

Sample tyre surface mesh, for R = 1, w = 0.5, R_c = 0.125, Δ = 0.0625. There are 2018 nodes and 4032 elements.

3.3 GROUND-PLANE REPRESENTATION

The effect of the ground plane is accounted for via the image theorem; a second body is generated by reflecting the nodes of the tyre representation through z = 0. In principle, this approach also demands a second exterior source, at the image location of the first. However, the far-field form discussed in Section 2.3 is unaffected, as it already satisfies the condition of zero normal velocity on z = 0.

The presence of the ground plane also creates numerical difficulties on the contact line that it shares with the cylindrical geometry. To avoid such difficulties, the tyre is displaced upwards by 0.000625R (1% of the standard scale parameter value; see following section). The image body is similarly displaced downwards.

3.4 MESH RESOLUTION

There are two separate, albeit linked, issues in deciding on how fine a mesh is required: acoustic resolution and geometric resolution. For the former, Graf et al [1] and O'Boy [3] quote a minimum requirement of four nodes per acoustic wavelength. For the latter, it has been decided that the smallest belt width (without crown radius), w = 0.25R, should be resolved by four rings, and that the smallest crown radius, R_c = 0.0625R, by two. Choosing the scale parameter equal to 0.0625R leads to meshes satisfying these requirements.

Assuming an internodal distance the same as the scale parameter then gives a minimum of 6.7 nodes per acoustic wavelength (at the highest frequency considered, kR = 15; see Section 4.1). Although this is well above the minimum recommendation, convergence has been checked by running a higher-resolution case, with scale parameter 0.05R (giving 8.4 nodes per wavelength at kR = 15) for the narrowest tyre. The results for this case are compared with those for the standard resolution in Figure 3.4, across three receiver angles (0°, 45°, 90°). Visually, the calculated amplifications appear effectively identical. However, the peak centre-line level for the forward receiver location is 1.3dB greater for the higher-resolution case. Although this difference will be less at lower frequencies, and is likely to be significantly reduced when comparing across geometries using the same scale parameter, it should be borne in mind when considering the results presented in the following section.

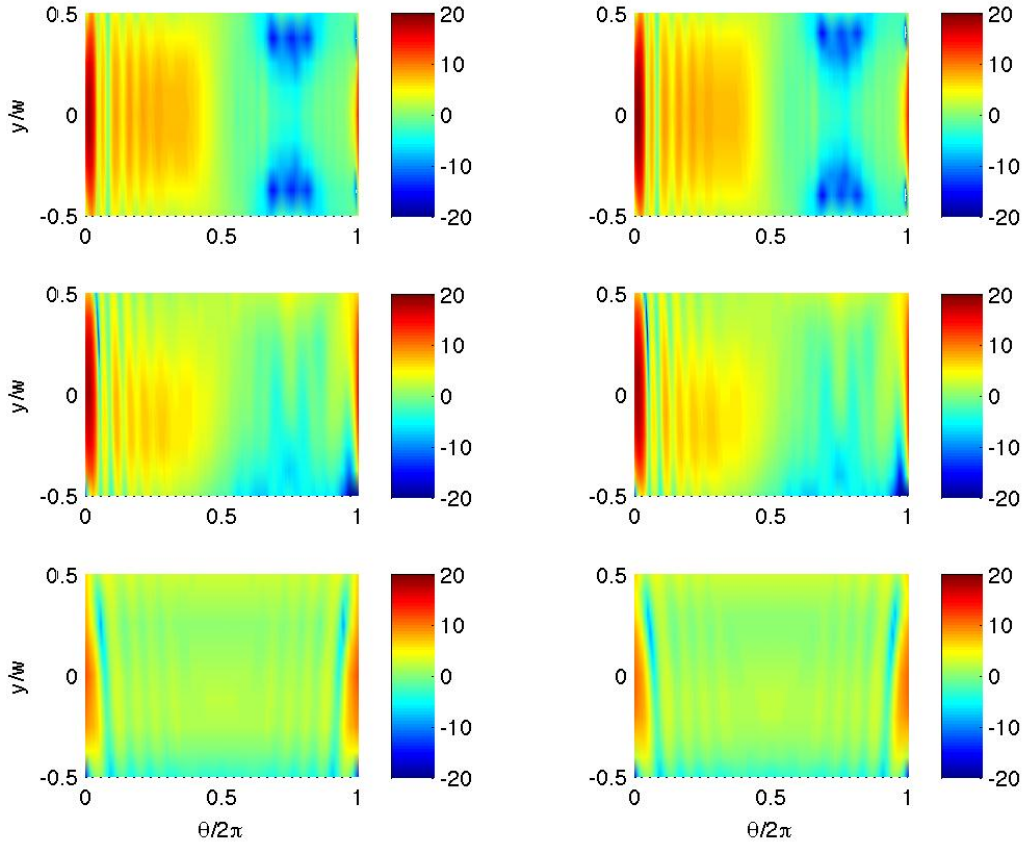

Figure 3.4

Horn amplification $20\log_{10}(|H|)$ for w/R = 0.25, kR = 15 and (top to bottom) receiver angle ϕ = 0°, 45°, 90°. Left: standard mesh, Δ = 0.0625R, maximum for ϕ = 0 18.4dB; right: higher-resolution mesh, Δ = 0.05R, maximum for ϕ = 0 19.7dB.

4 RESULTS

4.1 TEST CASES

The first question to be considered is the frequency range of interest. Graf et al's results [1] suggest that, for sources close to the contact line between tyre and road, there is a limiting amplification, reached, for their geometry, at about 2.5kHz. This corresponds to a dimensionless frequency kR = 14.8. There is also a practical limit imposed by the numerical requirements of the BEM calculation, which are already demanding for the largest geometries considered here. They would become impossible to fulfil, on a desktop computer, for frequencies significantly above kR = 15 (due to the acoustic-wavelength resolution condition). Equally, there is a frequency below which the horn amplification is almost negligible. For Graf et al's tyre this is approximately 500Hz, corresponding to kR = 3.0. The dimensionless frequencies considered are thus 3, 6, 9, 12 and 15.

Next the far-field receiver directions must be specified. Clearly of interest are the fore and side directions (ϕ = 0° and 90°). The intermediate angle, ϕ = 45°, is also considered.

The remaining parameters are geometric: w/R and R_c/R. Typical road vehicle tyres have width somewhat greater than half their radius; here, then, w = 0.5R is taken as a central, reference, case. The effect of altering this parameter is investigated via calculations at half, and twice, the reference width, ie 0.25R and R.

The crown radius has a maximum value of 0.5w, in which case there is no flat belt region. The minimum (non-zero) value is set by the width of one of the rings making up the mesh (see Section 3.4), ie 0.0625R. Thus, for the widest tyre, cases with R_c/R = 0.0625, 0.125, 0.25 and 0.5 are computed. Fewer values can be considered for the narrower tyres; the first three and two only for w = 0.5R and 0.25R respectively. The (reference) case of zero crown radius (ie sharp shoulders) is also included for all widths.

4.2 REFERENCE CASE

The horn amplification for the reference geometry, from all points on the belt to a far-field observer in the forward direction, is shown in Figure 4.1. For each frequency, the belt is shown unwrapped, with the azimuthal coordinate plotted on the x axis, scaled so that it runs from 0 to 1. Hence (see Figure 3.2), the horn region facing the source is on the left of the plots; x-coordinates 0.25, 0.5 and 0.75 represent, respectively, the furthest

forward, highest, and furthest rearward points on the belt. The y axis represents the belt y coordinate, scaled by the overall width.

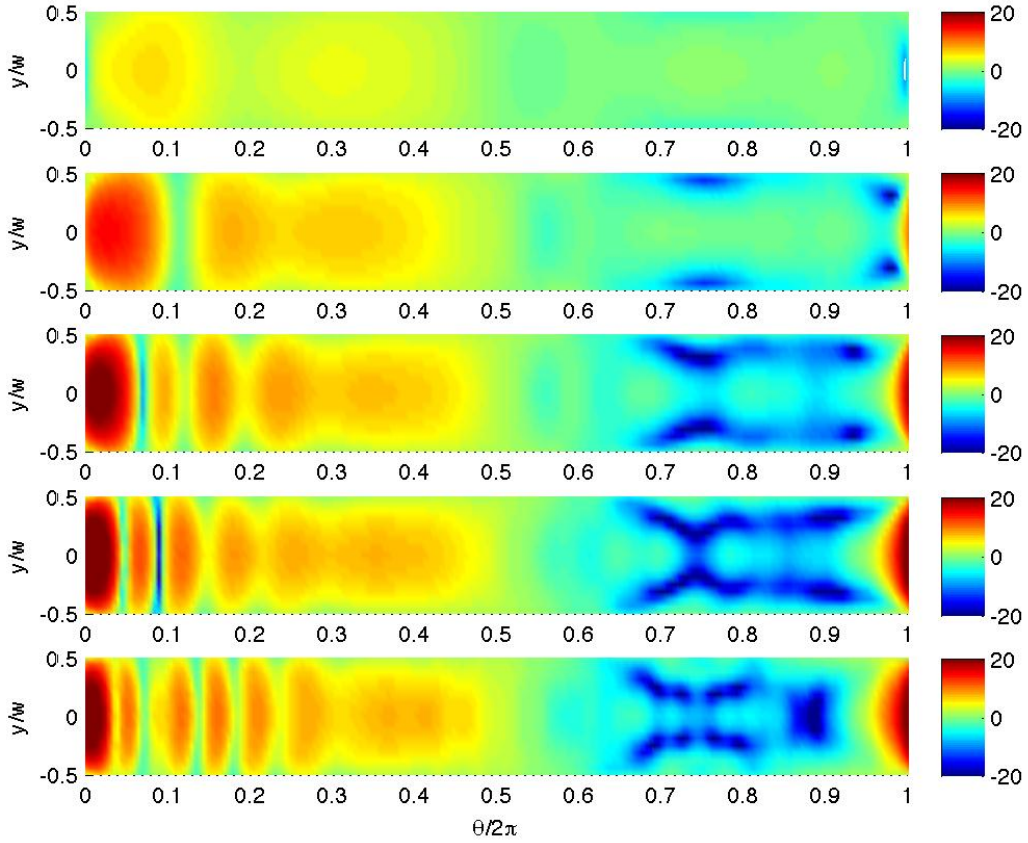

Figure 4.1

Horn amplification $20\log_{10}(|H|)$ for the reference tyre geometry (w/R = 0.5, R_c/R = 0) with (top to bottom) kR = 3, 6, 9, 12 and 15, and receiver angle $\phi = 0°$.

The most evident feature of the results is the expected increase in horn amplification with frequency. However, the structure of the plots also changes, with interference effects causing regions of maximum and minimum amplification. The first of these regions always includes the tyre base, and contains the points with greatest amplification. Furthermore, this amplification appears to tend to an approximately constant level at the higher frequencies. (Exact values of the peak amplification are given subsequently, in Table 4.1.) This feature is in agreement with Graf et al's finding that, for sources sufficiently close to the contact region, the amplification is effectively independent of source location [1]. Note also that the higher frequency results are consistent with the ray theory model of the horn effect [2]. In particular, sources on the rear part of the belt are 'shadowed' from the receiver, and have negative 'amplification'; there is also very little cross-belt variation away from the edges.

Figure 4.2 shows the corresponding results for the oblique receiver position, at $\phi = 45°$. The broad features, of increases in both amplification and number of interference

'lobes' with frequency, are unchanged. However, there is now a clear cross-belt structure at higher frequencies. Peak amplifications are slightly lower than for the forward receiver, but remain at very significant levels.

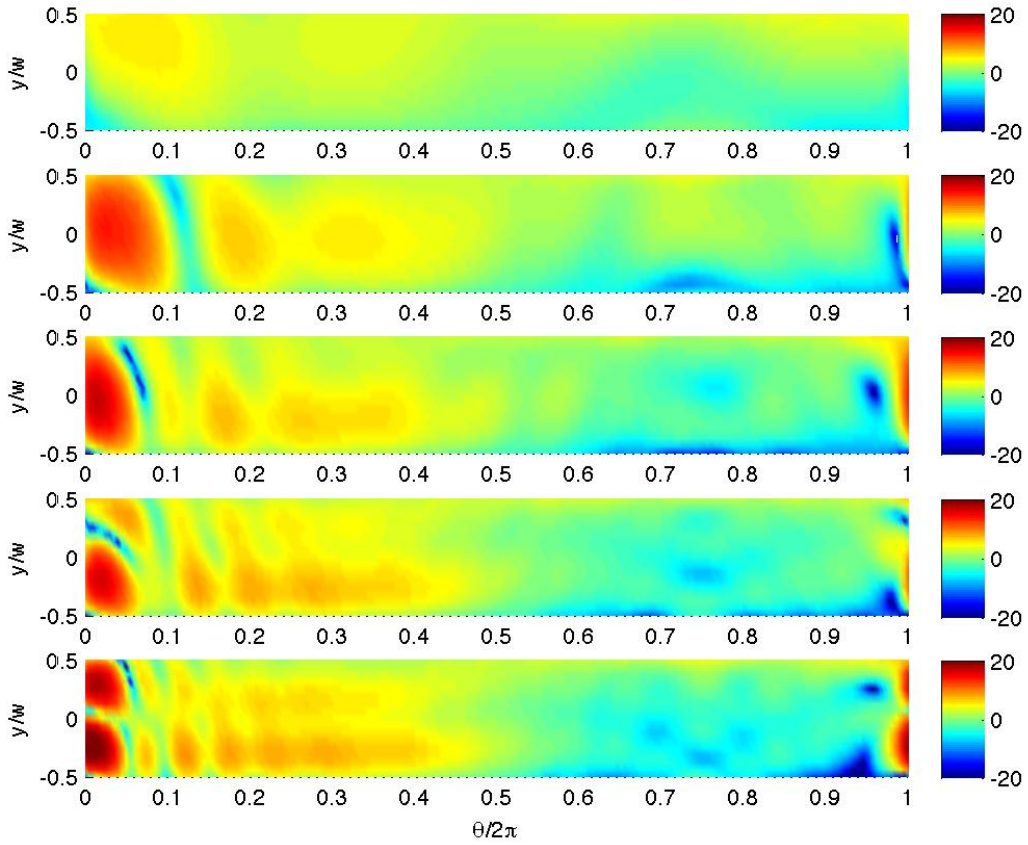

Figure 4.2

Horn amplification $20\log_{10}(|H|)$ for the reference tyre geometry ($w/R = 0.5$, $R_c/R = 0$) with (top to bottom) $kR = 3, 6, 9, 12$ and 15, and receiver angle $\phi = 45°$.

Finally, Figure 4.3 shows the results for the side-on receiver ($\phi = 90°$). Here there is a marked difference, both in amplification levels and in the extent of regions with high amplification. While the horn effect is still unlikely to be negligible for this observer location, it will be considerably less important than for listeners in the forward arc.

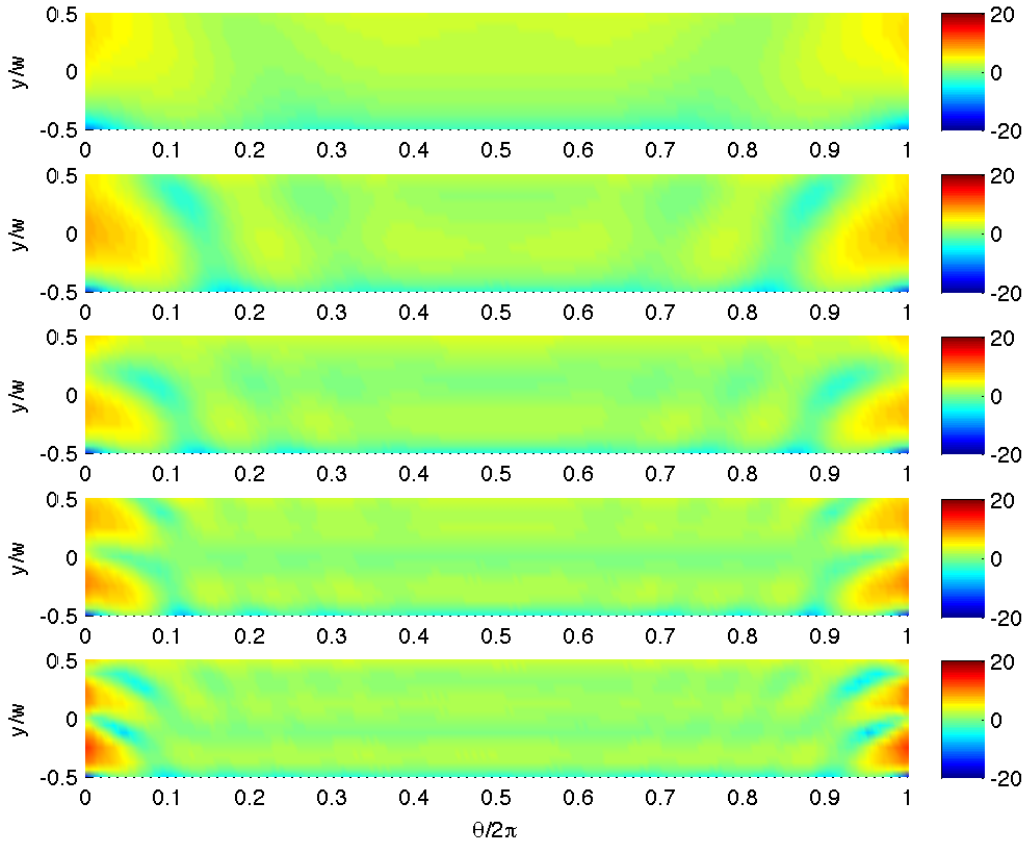

Figure 4.3

Horn amplification $20\log_{10}(|H|)$ for the reference tyre geometry (w/R = 0.5, R_c/R = 0) with (top to bottom) kR = 3, 6, 9, 12 and 15, and receiver angle $\phi = 90°$.

4.3 EFFECT OF WIDTH

In this section, the results for tyres of zero crown radius and varying widths are compared. Figure 4.4 shows the horn amplification from belt sources to a forward receiver, for w/R = 0.25, 0.5 and 1. (Note that colour bars are henceforth omitted to make better use of the plotting area; all plots have the same colour scale as Figures 4.1–4.3.) It is immediately evident that the belt width has a highly significant influence on the horn amplification at the lower frequencies, with wider tyres radiating noise much more efficiently. This observation is consistent with the predictions of the low-frequency asymptotic analysis presented by Kuo et al [2]. As the frequency increases, the differences become less marked. Such behaviour is to be expected, as a ray theory analysis for the centre-line sources would predict, to leading order, an amplification independent of belt width. This appears to be almost the case for the two wider tyres by kR = 12; the narrower, however, has not yet reached the ray-theory limit and remains significantly quieter. What can be said is that all three widths show a more-or-less identical azimuthal structure in the locations of their maxima and minima, and this observation also applies at the lower frequencies. One can therefore

conclude that the dimensionless frequency kR is the appropriate scaling parameter for this feature.

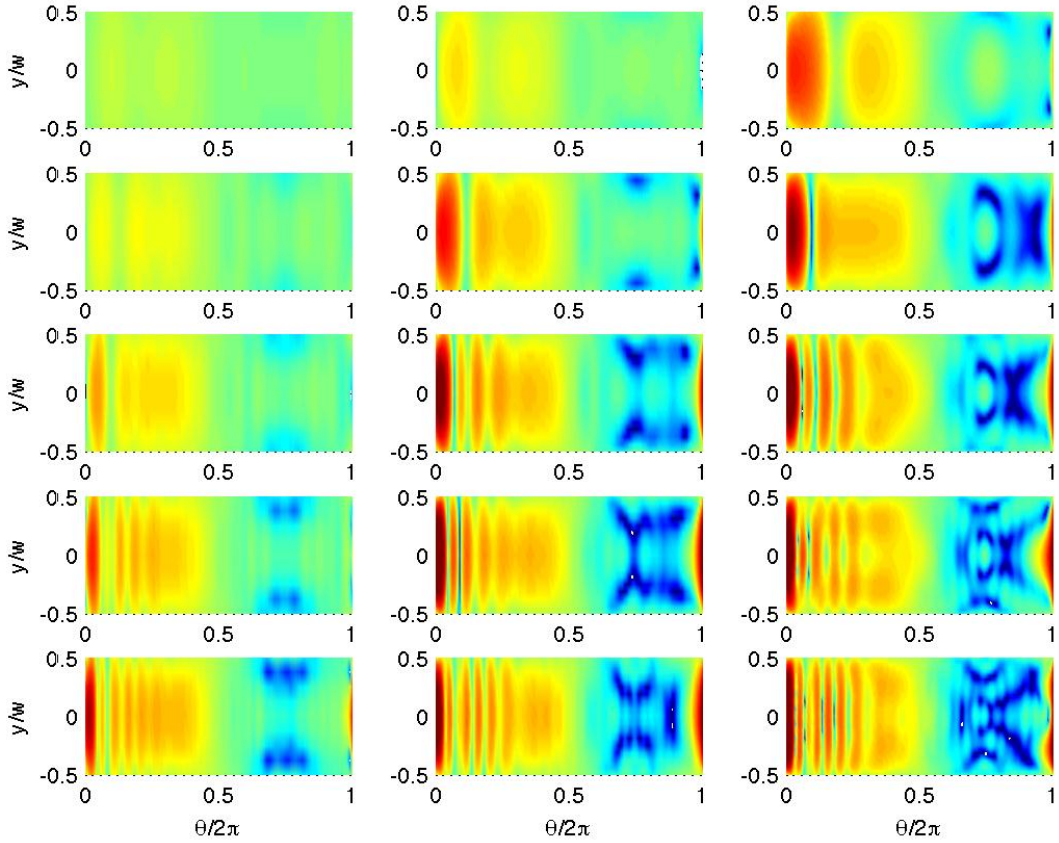

Figure 4.4

Horn amplification $20\log_{10}(|H|)$ for a sharp-edged tyre geometry ($R_c/R = 0$) with: (top to bottom) kR = 3, 6, 9, 12 and 15; (left to right) w/R = 0.25, 0.5 and 1; receiver angle $\phi = 0°$.

Peak amplification values for the forward receiver case are given below, in Table 4.1. These data substantiate the observations made from Figure 4.4, namely that the influence of width on peak amplification is greatest at low frequencies, and becomes effectively negligible at high enough frequency, with 'high enough' depending on the ratio of width to acoustic wavelength. Note also that peak values correlate quite well with kw (cf, for example, the kw = 3 data: kR = 3, 6 and 12 with w/R = 1, 0.5 and 0.25).

Table 4.1 Peak values of horn amplification $20\log_{10}(|H|)$ for a sharp-edged tyre geometry ($R_c/R = 0$) with receiver angle $\phi = 0°$.

w/R	kR = 3	kR = 6	kR = 9	kR = 12	kR = 15
0.25	2.5	4.5	8.7	13.6	18.4
0.5	5.9	14.9	21.3	24.8	23.0
1	13.5	19.6	23.0	24.2	22.3

The corresponding results for the other two receiver locations are presented in Figures 4.5 and 4.6. The observations made for the forward receiver location apply broadly unchanged to the oblique receiver case, with the additional point that the cross-belt structure noted previously has a predictable dependence on width. However, the side-on receiver case exhibits some important differences. While the narrower tyre remains the least efficient at radiating low-frequency sound, the differences between the three geometries are much smaller than previously, and peak amplification values at the higher frequencies are not greatly different. These features, though, are secondary in the overall context of the horn effect, given the generally low amplification levels for the side-on receiver.

Finally, an interesting feature of the narrowest geometry results is that the peak amplification at a given frequency is no longer necessarily found with a forward receiver location. This is a reflection of the fact that the mitigating effect of reducing the width is strongest for $\phi = 0°$.

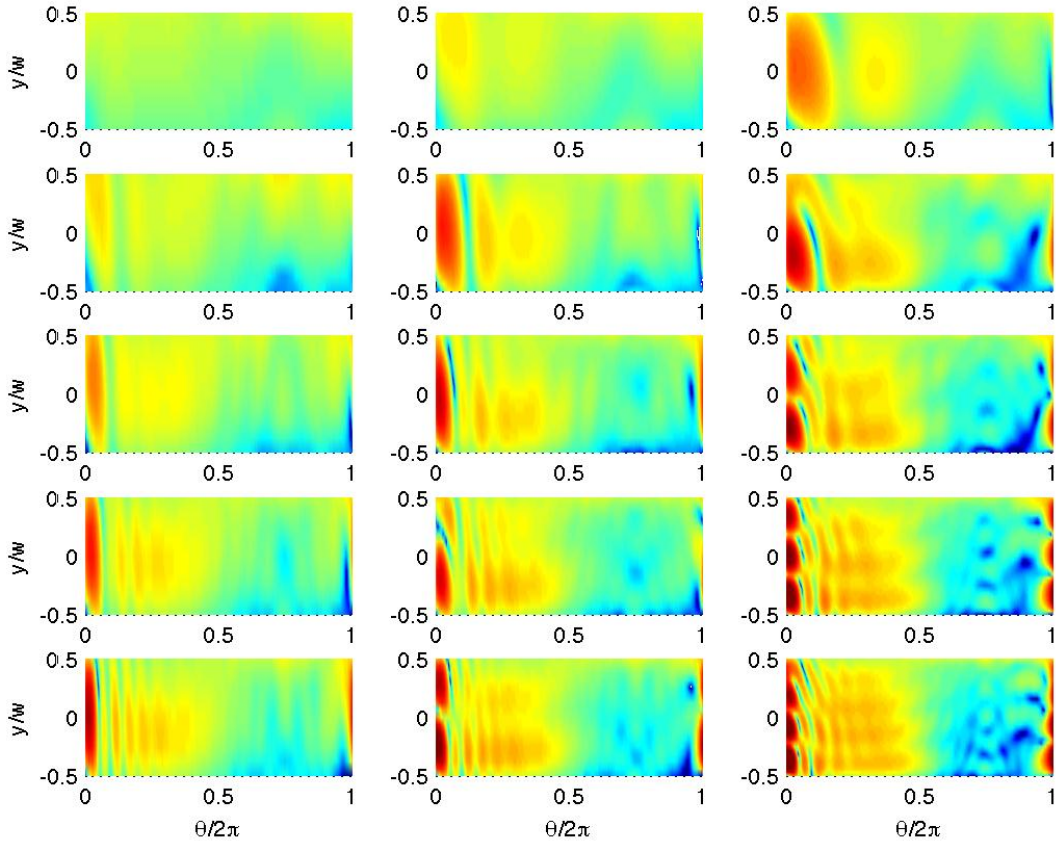

Figure 4.5

Horn amplification $20\log_{10}(|H|)$ for a sharp-edged tyre geometry ($R_c/R = 0$) with: (top to bottom) kR = 3, 6, 9, 12 and 15; (left to right) w/R = 0.25, 0.5 and 1; receiver angle $\phi = 45°$.

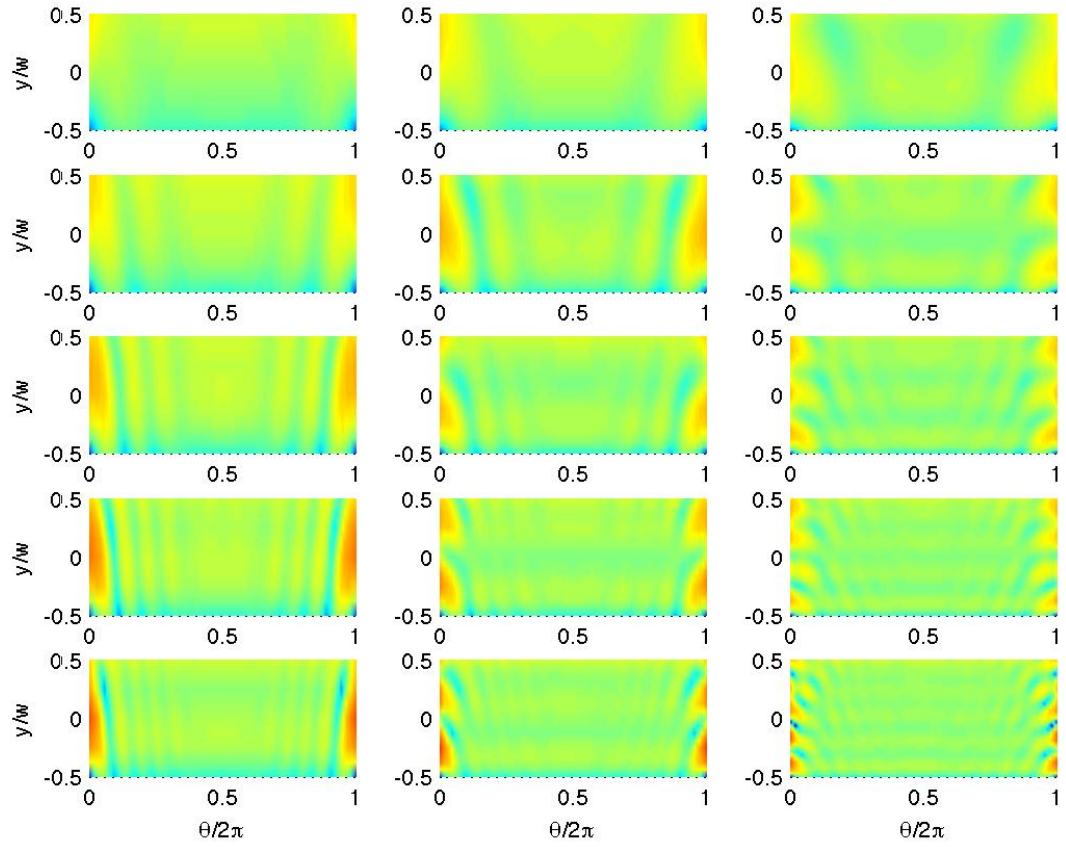

Figure 4.6

Horn amplification $20\log_{10}(|H|)$ for a sharp-edged tyre geometry ($R_c/R = 0$) with: (top to bottom) kR = 3, 6, 9, 12 and 15; (left to right) w/R = 0.25, 0.5 and 1; receiver angle $\phi = 90°$.

4.4 EFFECT OF CROWN RADIUS

The impact of radiusing the tyre crown is first considered for the reference width of 0.5R. The horn amplification for all four applicable radii (0, 0.0625R, 0.125R and 0.25R) is plotted, for the forward receiver location, in Figure 4.7. At the lowest frequency, kR = 3, where the tyre is still close to being acoustically compact, the modification has rather little effect. However, at the higher frequencies, it is clear that the spanwise extent of the regions of maximum amplification is progressively reduced as the crown radius increases. The peak level does not necessarily drop significantly at the same time, although by $R_c = 0.25R$ (a fully-rounded belt) it is always greatly reduced from the sharp-edged value.

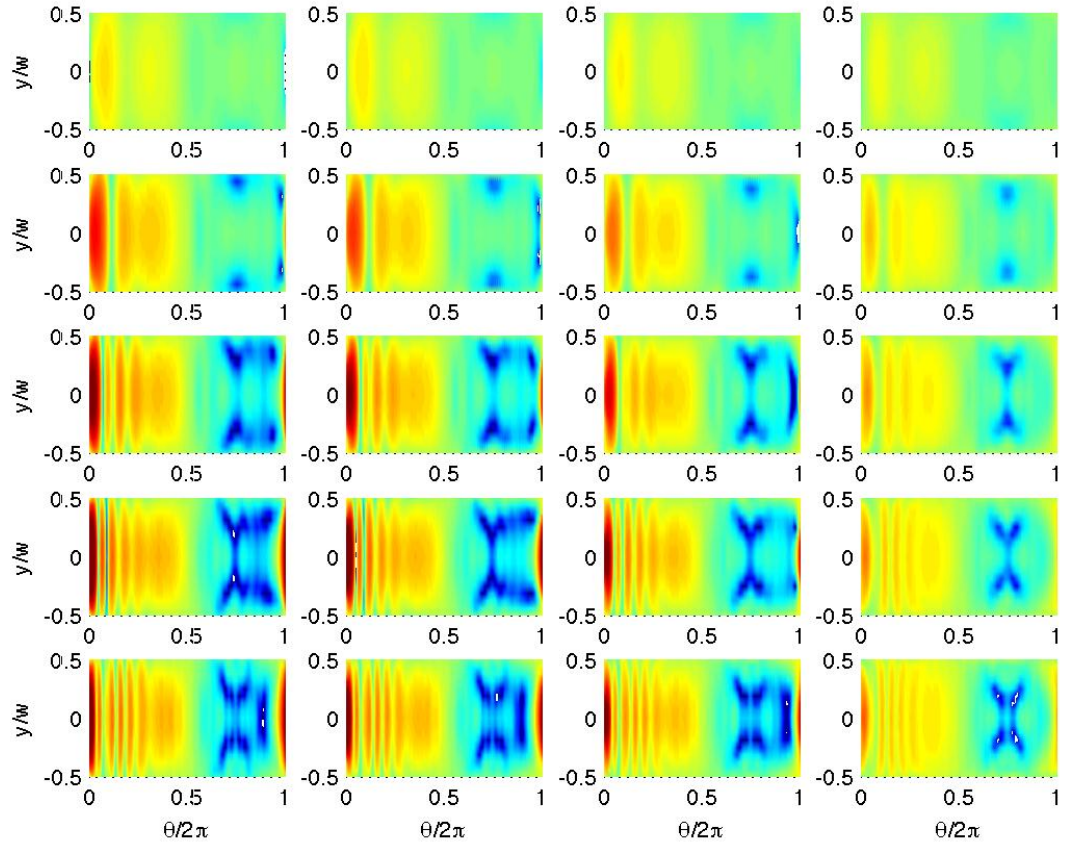

Figure 4.7

Horn amplification $20\log_{10}(|H|)$ for the reference-width tyre geometry (w/R = 0.5) with: (top to bottom) kR = 3, 6, 9, 12 and 15; (left to right) R_c/R = 0, 0.0625, 0.125, and 0.25; receiver angle ϕ = 0°.

The corresponding results for the oblique and side-on receivers are plotted in Figures 4.8 and 4.9. Qualitatively, Figure 4.8 shows the same behaviour as for the forward receiver. Figure 4.9, however, introduces a new feature; increasing amplification as the crown radius increases. This is because the crown region now, to some extent, faces the receiver, allowing it to communicate much more efficiently. The reduced forward amplification has been obtained at the cost of a penalty side-on. Thus, for the fully-rounded geometry, the peak amplifications are comparable with those experienced by the forward observer. Nonetheless, their levels remain significantly lower than for the sharp-edged tyre with a forward observer.

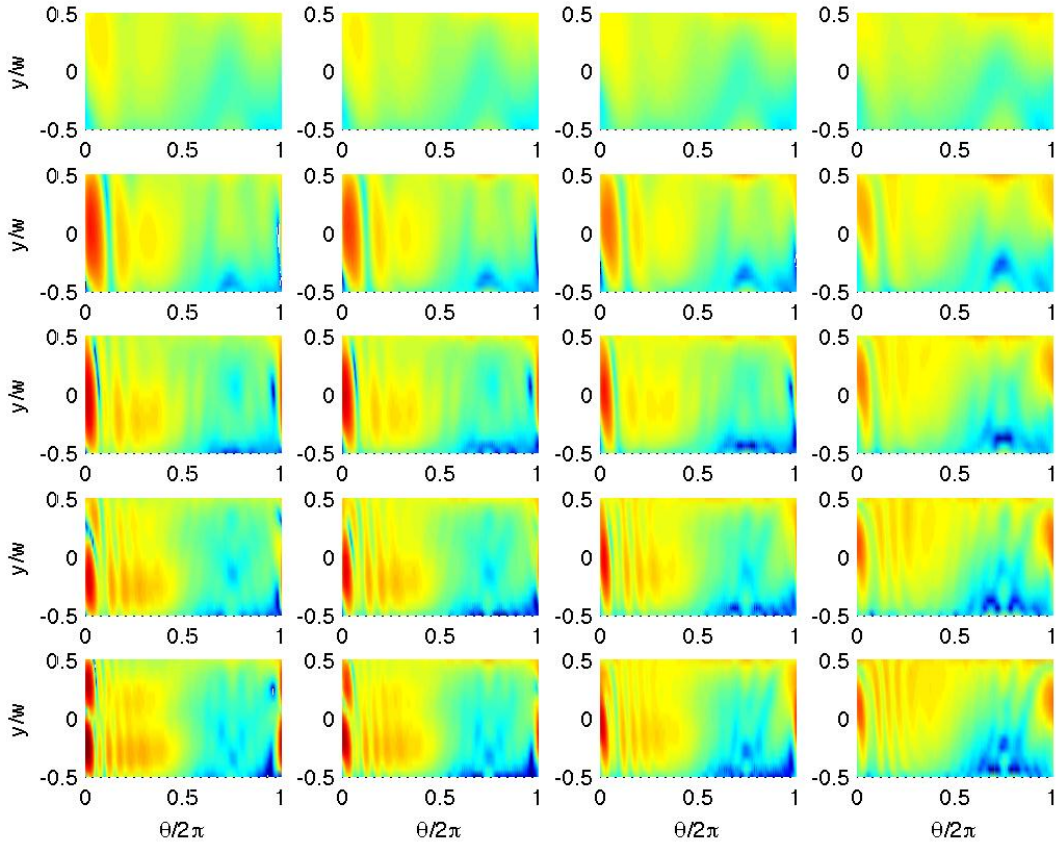

Figure 4.8

Horn amplification $20\log_{10}(|H|)$ for the reference-width tyre geometry (w/R = 0.5) with: (top to bottom) kR = 3, 6, 9, 12 and 15; (left to right) R_c/R = 0, 0.0625, 0.125, and 0.25; receiver angle ϕ = 45°.

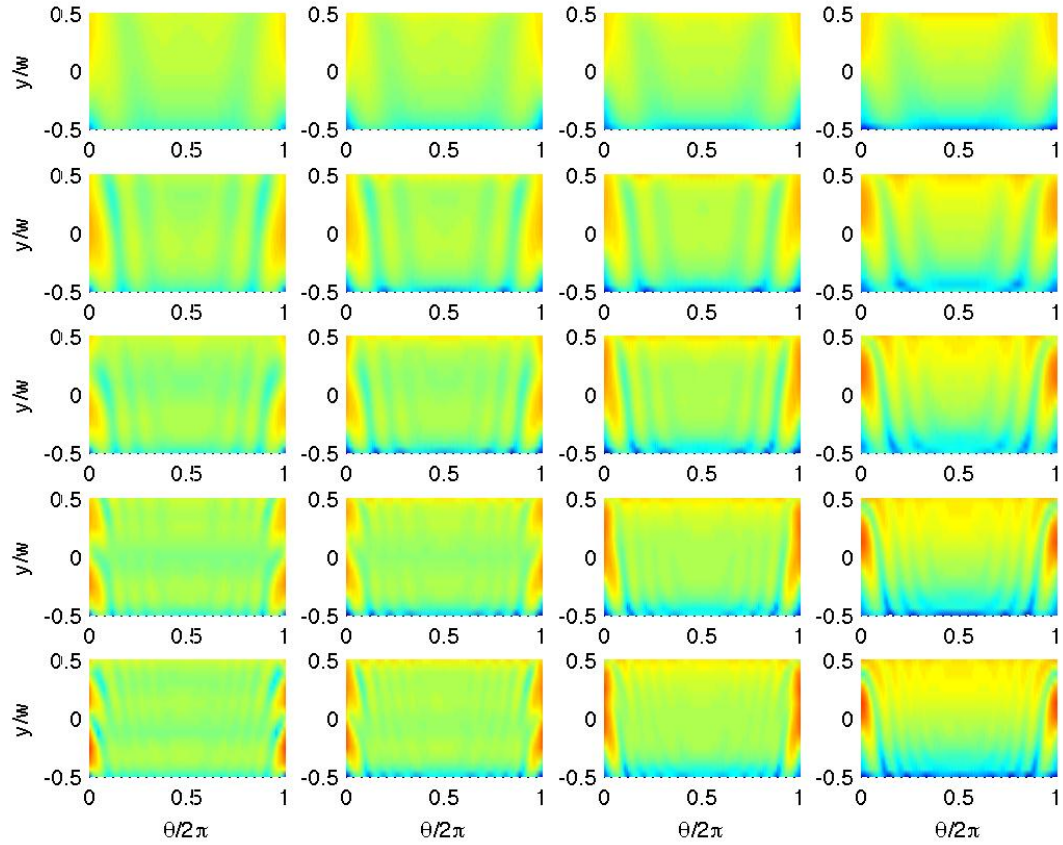

Figure 4.9

Horn amplification $20\log_{10}(|H|)$ for the reference-width tyre geometry (w/R = 0.5) with: (top to bottom) kR = 3, 6, 9, 12 and 15; (left to right) R_c/R = 0, 0.0625, 0.125, and 0.25; receiver angle ϕ = 90°.

The corresponding plots for the narrow and wide geometries are provided in the appendix. They show the same behaviour as for the reference-width case, with the important exception that the frequency at which radiusing can have a significant effect changes; for w = 0.25R it lies between kR = 6 and 9, whereas for w = R it is below kR = 3. This implies that the measure of tyre compactness for this feature is kw, rather than kR, and that the transition occurs somewhere between kw = 1.5 and 2.25.

The above observations are supported by the maximum amplifications for the forward receiver location. These are given, frequency by frequency, in Tables 4.2–4.6.

Table 4.2 Peak values of horn amplification $20\log_{10}(|H|)$ for varying crown radii at kR = 3, with receiver angle ϕ = 0°.

w/R	R_c = 0	R_c = 0.0625R	R_c = 0.125R	R_c = 0.25R	R_c = 0.5R
0.25	2.5	2.4	2.2	—	—
0.5	5.9	5.6	5.2	4.5	—
1	13.5	13.1	12.3	10.6	7.3

Table 4.3 Peak values of horn amplification $20\log_{10}(|H|)$ for varying crown radii at kR = 6, with receiver angle $\phi = 0°$.

w/R	$R_c = 0$	$R_c = 0.0625R$	$R_c = 0.125R$	$R_c = 0.25R$	$R_c = 0.5R$
0.25	4.5	4.0	3.6	—	—
0.5	14.9	13.0	10.5	7.2	—
1	19.6	19.5	19.3	18.3	10.3

Table 4.4 Peak values of horn amplification $20\log_{10}(|H|)$ for varying crown radii at kR = 9, with receiver angle $\phi = 0°$.

w/R	$R_c = 0$	$R_c = 0.0625R$	$R_c = 0.125R$	$R_c = 0.25R$	$R_c = 0.5R$
0.25	8.7	6.8	5.0	—	—
0.5	21.3	20.0	16.3	9.1	—
1	23.0	23.0	22.8	21.9	12.0

Table 4.5 Peak values of horn amplification $20\log_{10}(|H|)$ for varying crown radii at kR = 12, with receiver angle $\phi = 0°$.

w/R	$R_c = 0$	$R_c = 0.0625R$	$R_c = 0.125R$	$R_c = 0.25R$	$R_c = 0.5R$
0.25	13.6	9.5	6.5	—	—
0.5	24.8	24.5	20.9	10.1	—
1	24.2	24.6	24.5	23.0	13.8

Table 4.6 Peak values of horn amplification $20\log_{10}(|H|)$ for varying crown radii at kR = 15, with receiver angle $\phi = 0°$.

w/R	$R_c = 0$	$R_c = 0.0625R$	$R_c = 0.125R$	$R_c = 0.25R$	$R_c = 0.5R$
0.25	18.4	11.8	7.1	—	—
0.5	23.0	23.3	21.3	11.6	—
1	22.3	21.6	21.9	21.6	14.5

5 DISCUSSION

In this section, the implications of the results for vehicle tyres in general, and truck tyres in particular, are discussed. First, only the geometries with zero crown radius are considered. Then the effects of rounding the shoulder region are taken into account.

5.1 SHARP-SHOULDERED GEOMETRIES

For $R_c = 0$, the forward and 45° receiver locations are unquestionably more critical than side-on, and the behaviour of both cases is well represented by the former. Therefore the discussion here is based on the $\phi = 0°$ results.

The data of Section 4.3 show that the peak amplification level increases strongly with width, at least until the tyre is wide enough that edge effects have no influence on the belt centre-line. Subsequently the peak level remains more-or-less constant, but the cross-belt extent of the peak amplification region grows.

Apparently, then, the required strategy for a quiet tyre is clear: minimise its width. However, this neglects the practical implications of the corresponding decrease in contact-patch area. Even if it were mechanically feasible to build a tyre capable of bearing the increased contact-patch pressure, the amplitude of the belt vibrations would increase. A fairer comparison is to consider decreasing w and increasing R such that the product wR (which one would expect to be approximately proportional to contact-patch area) remains constant. At a given (dimensional) frequency, this corresponds to maintaining $(w/R)(kR)^2$ constant. Figures 5.1 and 5.2 show the two comparisons satisfying this condition that can be extracted from the current data set: $w/R = 0.25$, $kR = 6$ against $w/R = 1$, $kR = 3$, and $w/R = 0.25$, $kR = 12$ against $w/R = 1$, $kR = 6$.

In both cases, the benefit of the narrower belt clearly outweighs any potential disadvantages of moving to higher kR. In practice, the characteristics of the vibration field will also play a part. While this aspect is outside the scope of the current investigation, one might expect the region of significant vibration amplitudes to cover approximately the same azimuthal proportion of the belt in each case, and hence the same physical area. For purely uncorrelated vibrations, this would then imply that the average horn amplification over the relevant area is the key noise parameter, supporting the initial claim. Real vibrations will be correlated to some extent, in which case the phase of the amplification will also be important. In certain, special, cases this might lead to lower noise from the wider tyre, but such unusual instances are unlikely to be robust to, for example, changes in vehicle speed. It can therefore be concluded

with some confidence that narrower tyres are preferable to wider, even when practical, load-bearing, considerations are accounted for.

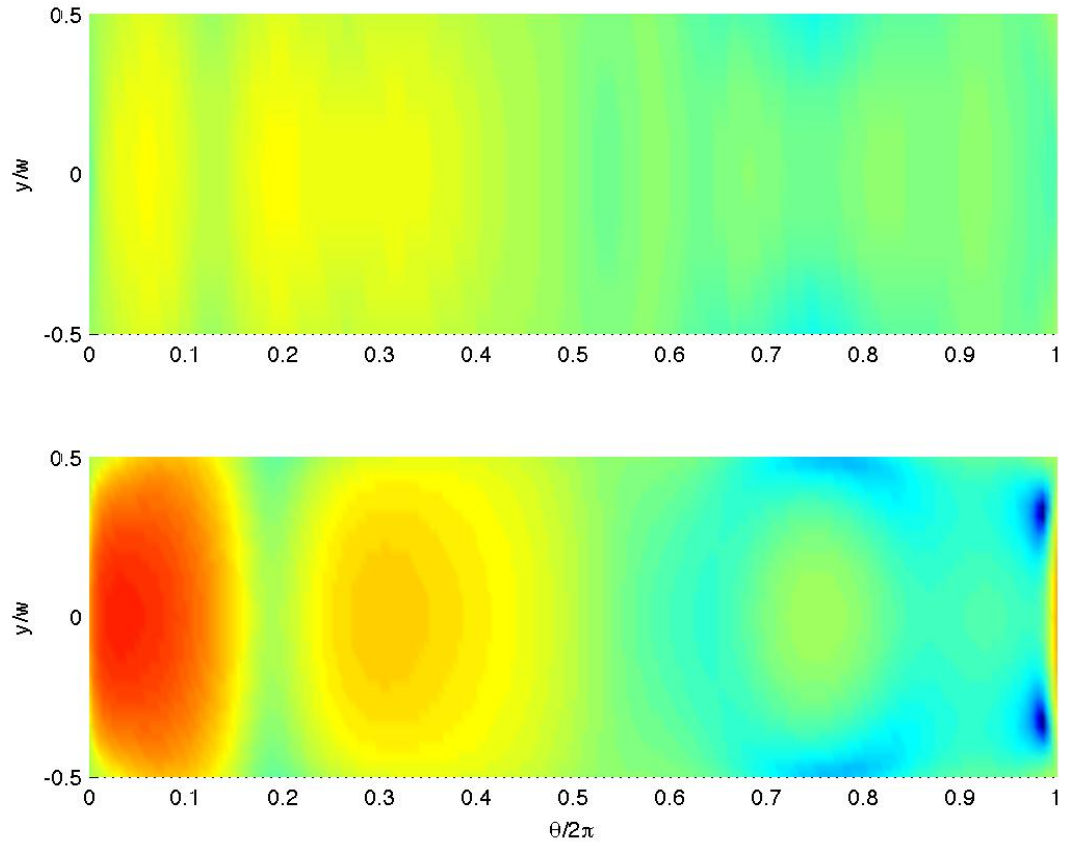

Figure 5.1

Horn amplification $20\log_{10}(|H|)$ for the narrow (w/R = 0.25, top) and wide (w/R = 1, bottom) tyre geometries with (respectively) kR = 6 and 3; receiver angle $\phi = 0°$.

Current truck tyres are typically around 1m in diameter, giving kR ≅ 9 at the frequency where human sound sensitivity peaks, 1kHz. Thus Figure 5.2 is of most relevance to the specific application of interest here. Although the benefit of width reduction appears less marked than in Figure 5.1, the peak level is still lowered by 6dB. Given the behaviour observed in Section 4.2, one would expect this difference to reduce with increasing frequency, until eventually both peak amplifications were the same. However, even if this were at frequencies where the vibration level and human sensitivity were still non-negligible, the wider tyre would maintain its peak amplification across a much greater cross-belt range than the narrower, and would therefore still be significantly noisier. The general recommendation to minimise tyre width would thus deliver reductions in noise from heavy vehicles in the relevant frequency range.

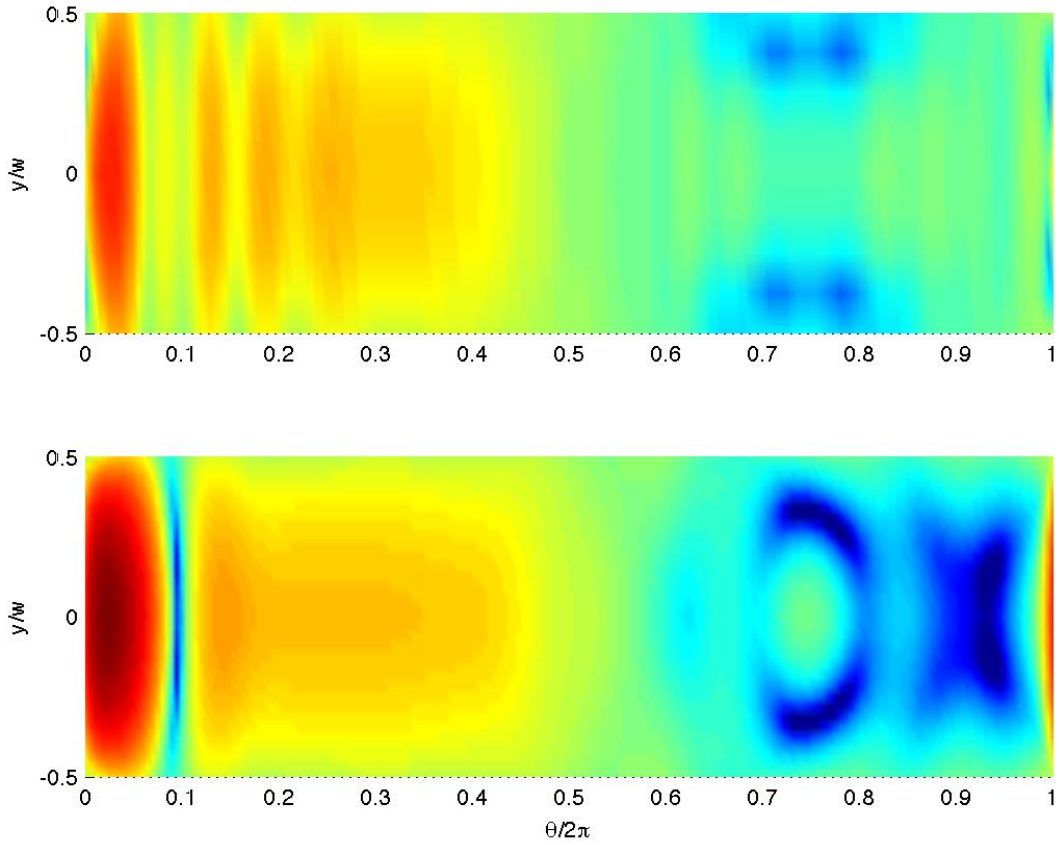

Figure 5.2

Horn amplification $20\log_{10}(|H|)$ for the narrow (w/R = 0.25, top) and wide (w/R = 1, bottom) tyre geometries with (respectively) kR = 12 and 6; receiver angle $\phi = 0°$.

5.2 CROWN RADIUS RECOMMENDATIONS

As in the previous section, attention will be restricted to results for $\phi = 0°$. However, it should be borne in mind that benefits for this case may be offset by increased side-on radiation as R_c is increased.

The results of Section 4.4 showed that, for a tyre of given overall width, radiusing the crown region is potentially beneficial, although this potential is only significantly realised if the radiused region represents a substantial proportion of the overall width. The limit is the motorcycle-style tyre, with $R_c = w/2$. This, however, is not a practical possibility for four-wheeled vehicles, due to wear requirements. Furthermore, one would expect that a crown-radiused tyre with the same load-bearing capacity as a sharp-shouldered geometry should have the same *belt* width, ie that the comparison should be between tyres with the same value of $w - 2R_c$. Two such comparisons can be made from the

current data set: w/R = 0.25, R_c = 0 against w/R = 0.5, R_c = 0.125R, and w/R = 0.5, R_c = 0 against w/R = 1, R_c = 0.25R. They are shown in Figures 5.3 and 5.4.

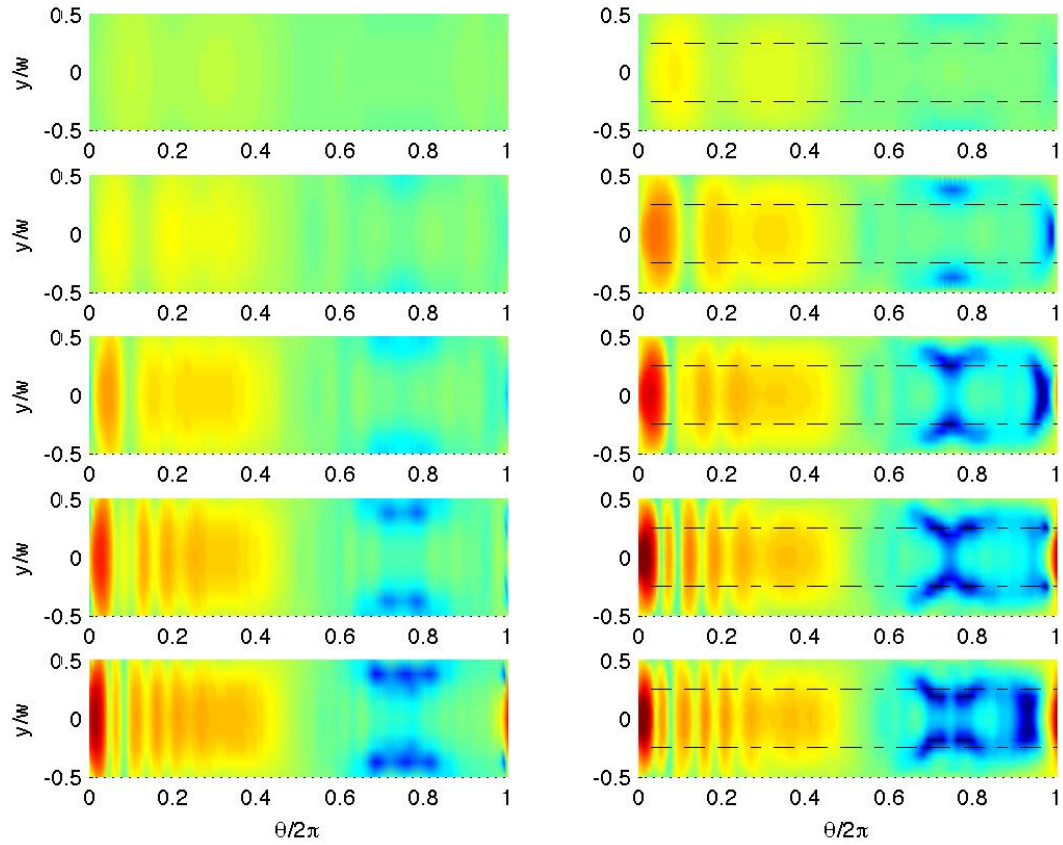

Figure 5.3

Horn amplification $20\log_{10}(|H|)$ for belt width 0.25R, with: (top to bottom) kR = 3, 6, 9, 12 and 15; w/R = 0.25, R_c/R = 0 (left) and w/R = 0.5, R_c/R = 0.125 (right); receiver angle ϕ = 0°. Dashed lines on right-hand plots indicate extent of (flat) belt region.

In discussing these figures, the relevant comparison is between the flat-belt regions, represented by the whole of the plots on the left, but only the parts between dashed lines on the right. For the smaller width belt (Figure 5.3), it is then immediately clear that the sharp-shouldered tyre with lower overall width is superior in noise performance. In the wider belt case the distinction is less marked, because the frequency where the centre-line peak amplification 'saturates' is lower, at kR = 9. However, careful examination shows that the cross-belt extent of the peak amplification is slightly lower for the sharp-shouldered tyre, so it would remain superior, albeit probably only marginally so. At the lower frequencies, it is still clearly preferable.

A definitive evaluation of the effect of crown radiusing on the side-on receiver is not possible from these results, since the sidewall contribution has not been considered. However, given the adverse effects noted in Section 4.4, it seems likely that the introduction of radiusing is, at best, neutral for this receiver location, and is probably

detrimental. While the side-on amplification will, as noted previously, be lower than for the forward and oblique receivers, it cannot wholly be ignored, as in practice listeners at this angle will typically be closer to vehicles.

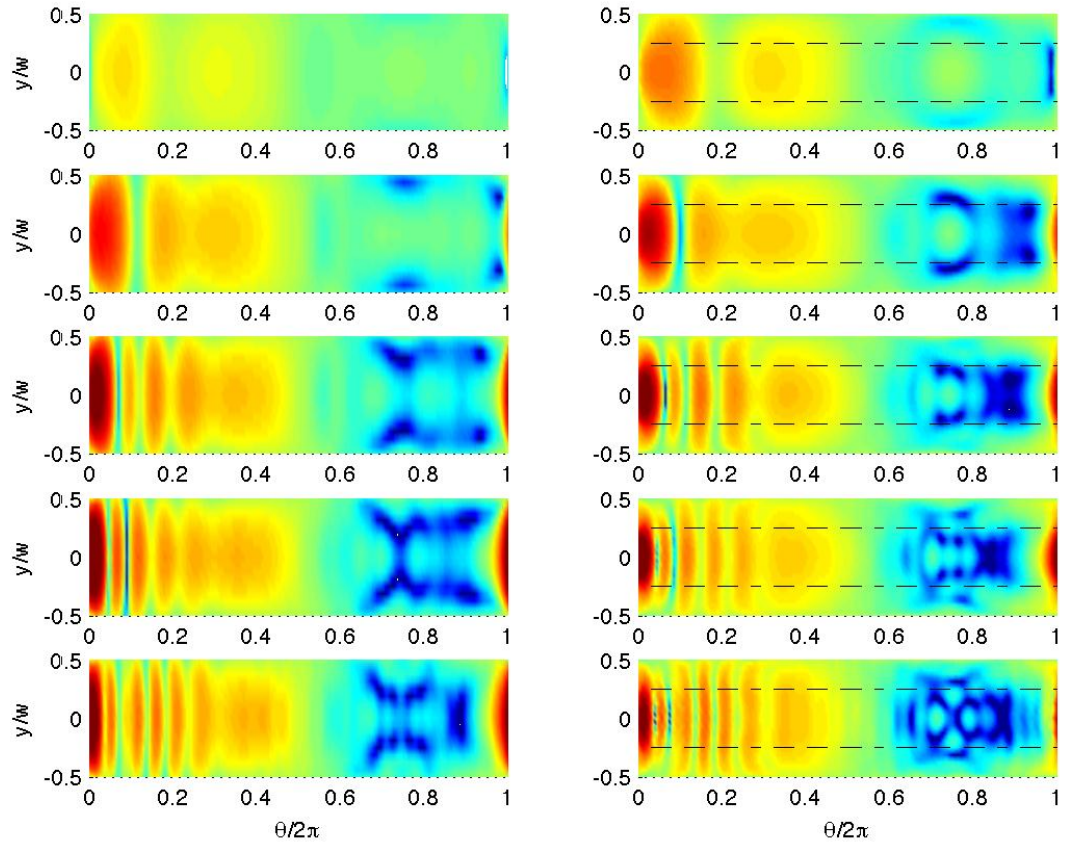

Figure 5.4

Horn amplification $20\log_{10}(|H|)$ for belt width 0.5R, with: (top to bottom) kR = 3, 6, 9, 12 and 15; w/R = 0.5, $R_c/R = 0$ (left) and w/R = 1, $R_c/R = 0.25$ (right); receiver angle $\phi = 0°$. Dashed lines on right-hand plots indicate extent of (flat) belt region.

To summarise: the results in this section demonstrate unambiguously that, for the same belt width, there is no benefit for the forward (and, by implication, the oblique) receiver location in radiusing the tyre crown; in fact, the opposite is true. Quantitative evaluation of the impact on a listener to the side is beyond the scope of this report, but it is highly unlikely that it is in any way beneficial, and it is probably detrimental. These conclusions apply not just to trucks, but to all road vehicles with belted tyres.

6 CONCLUSIONS

This report has considered the impact of tyre geometry on the acoustic amplification of noise sources on the tyre belt, with specific reference to the heavy vehicle application. The tyre has been represented by a generic, circular-cylinder, shape, with radius R, overall width w, and crown radius R_c. The source amplification from all points on the belt to three receiver locations—forward, oblique and side-on—has been calculated using the Boundary Element Method applied to a reciprocal configuration.

For the basic, sharp-shouldered shape ($R_c = 0$), the horn amplification increases from 0dB as the sound frequency rises and its wavelength decreases; simultaneously the number of azimuthal maxima and minima in the amplification also increases. The broad topology of this pattern is determined by the dimensionless frequency kR, where k is the acoustic wavenumber. The peak amplification is always found where the tyre belt approaches the ground plane. At sufficiently high frequencies, the peak value reaches almost 25dB; once such a level is attained, further increases in frequency lead to a cross-belt broadening of the peak-value region. Unlike the azimuthal topology, the peak amplification is governed by kw; its saturation corresponds to the tyre width becoming sufficiently large that it appears infinite from the point of view of sources on the centre-line.

The dependence of the peak amplification on kw means that the horn amplification is mitigated by a reduction in tyre width. This applies even after the peak value has saturated, because of the reduced cross-belt extent of the region where it is attained. In practice, it will probably be necessary to increase the tyre radius if it is to carry the same load with lower width. Nonetheless, even taking this requirement into account, width reduction can be expected to yield significant noise benefits.

Radiusing the crown region has little impact at lower frequencies, when the tyre width is smaller than the acoustic wavelength. At higher frequencies, it has a mitigating influence which becomes significant once the radiused region represents an appreciable proportion of the overall width. However, when compared against a sharp-shouldered tyre of the same width as the remaining, flat, belt region, the radiused geometry has significantly worse radiation characteristics.

In the light of these observations, vehicle tyres should be made as narrow as is practically possible, even if this necessitates a commensurate increase in their diameter. Crown radiusing is not essential, and should certainly not be employed if it implies an increase in the overall tyre width. Following these recommendations will lead to noise reductions across all frequencies, so they apply equally to truck and car tyres.

REFERENCES

1. R A G Graf, C-Y Kuo, A P Dowling and W R Graham. On the horn effect of a tyre/road interface, Part I: Experiment and computation. *Journal of Sound and Vibration*, 256, pp417-431, 2002.
2. R A G Graf, C-Y Kuo, A P Dowling and W R Graham. On the horn effect of a tyre/road interface, Part II: Asymptotic theories. *Journal of Sound and Vibration*, 256, pp433-445, 2002.
3. D J O'Boy. Changes in external noise from a tyre with smaller crown radius. *Deliverable 3.24*, QCITY project (FP6-516420).
4. A D Pierce. *Acoustics: an introduction to its physical principles and applications*, Acoustical Society of America, 1989. Chapter 4.
5. V Cutanda Henriquez and P M Juhl. OpenBEM: an open source Boundary Element Method software in acoustics. *Proceedings InterNoise 2010,* June 2010, Lisbon, Portugal.

APPENDIX

This appendix contains supplementary material for Section 4.4, on the effect of crown radius. Note that, for the widest geometry (w = R), two plots per source are required to cover the range of R_c. The case R_c = 0.125R is repeated in the second plot, for reference.

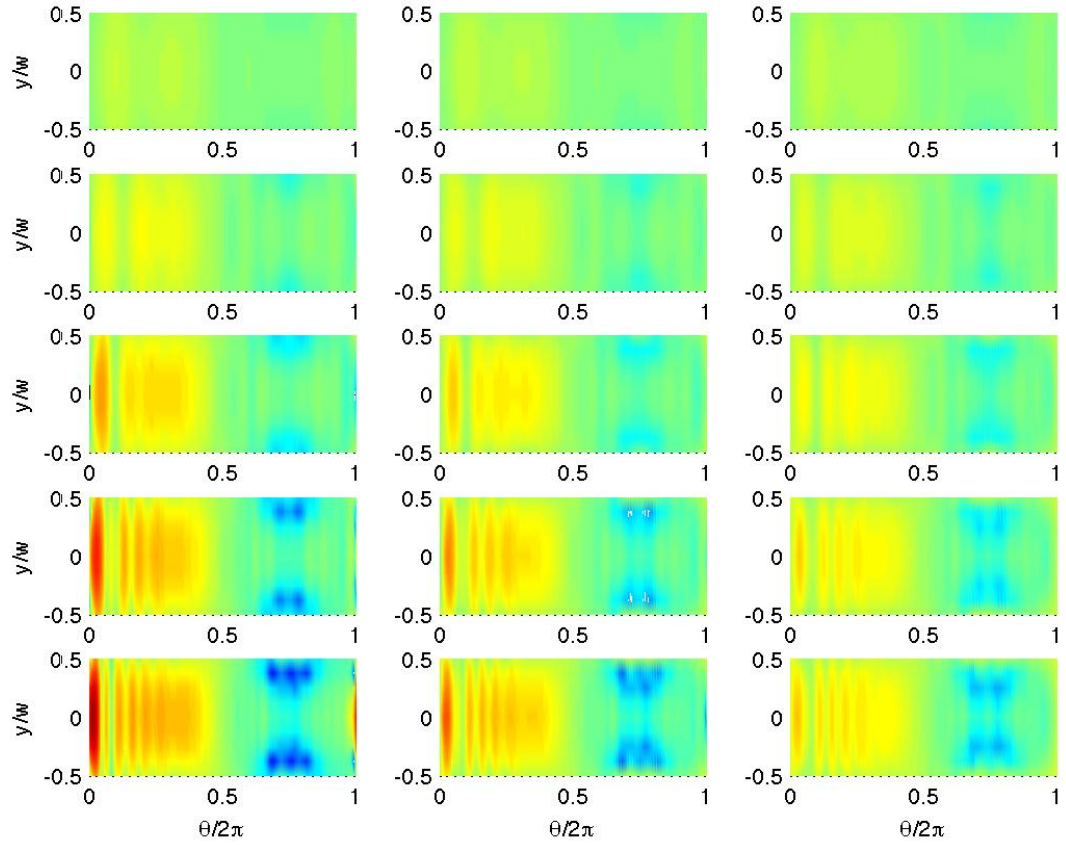

Figure A.1

Horn amplification $20\log_{10}(|H|)$ for the narrow tyre geometry (w/R = 0.25) with: (top to bottom) kR = 3, 6, 9, 12 and 15; (left to right) R_c/R = 0, 0.0625, and 0.125; receiver angle $\phi = 0°$.

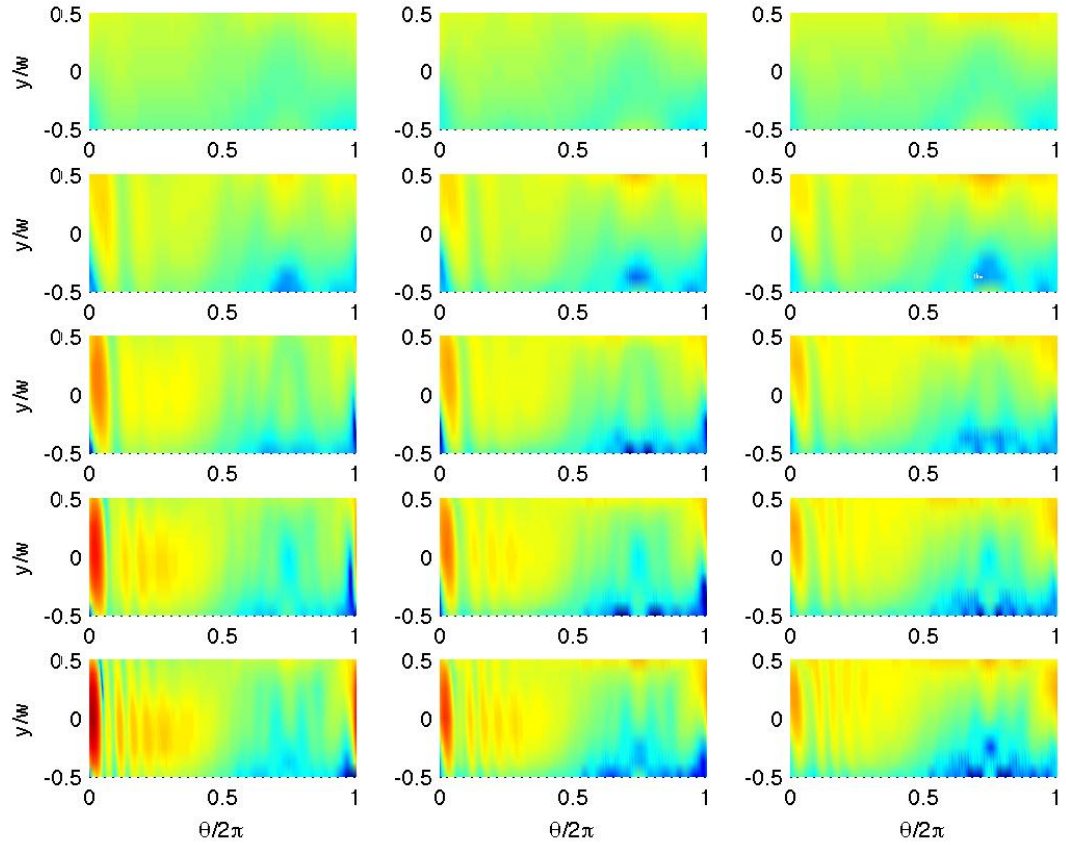

Figure A.2

Horn amplification $20\log_{10}(|H|)$ for the narrow tyre geometry (w/R = 0.25) with: (top to bottom) kR = 3, 6, 9, 12 and 15; (left to right) R_c/R = 0, 0.0625, and 0.125; receiver angle ϕ = 45°.

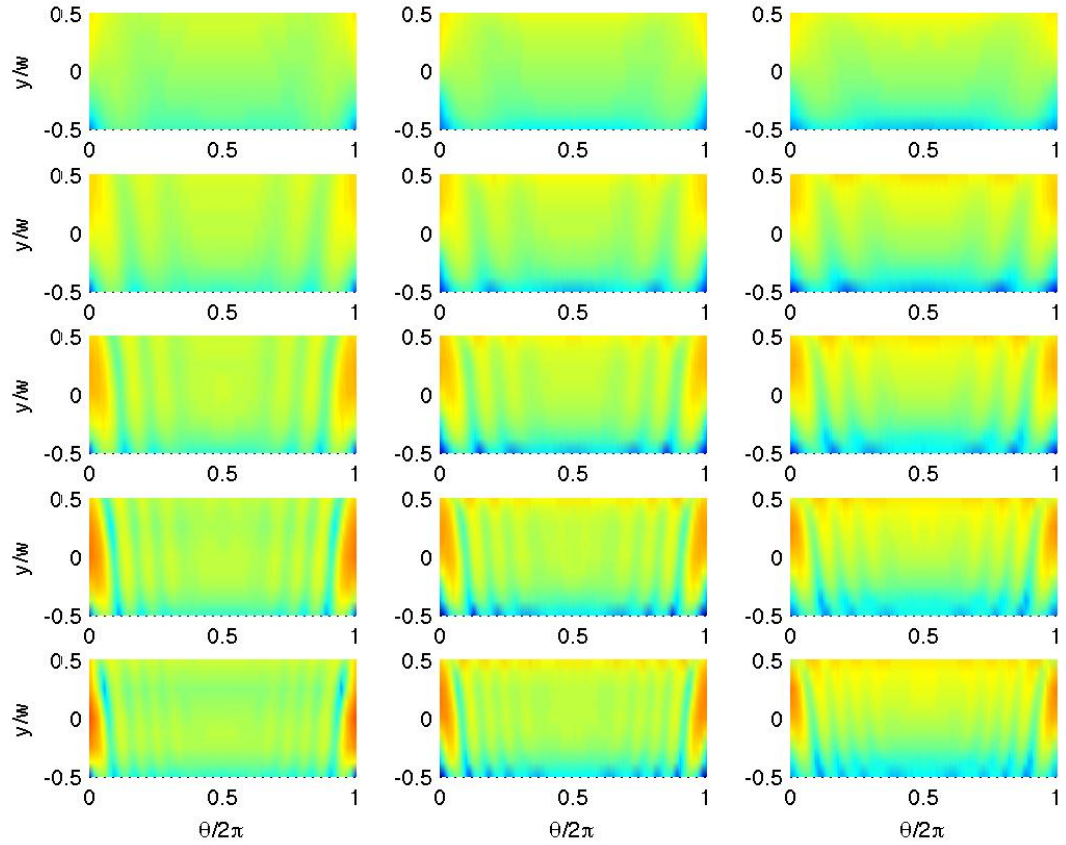

Figure A.3

Horn amplification $20\log_{10}(|H|)$ for the narrow tyre geometry (w/R = 0.25) with: (top to bottom) kR = 3, 6, 9, 12 and 15; (left to right) R_c/R = 0, 0.0625, and 0.125; receiver angle ϕ = 90°.

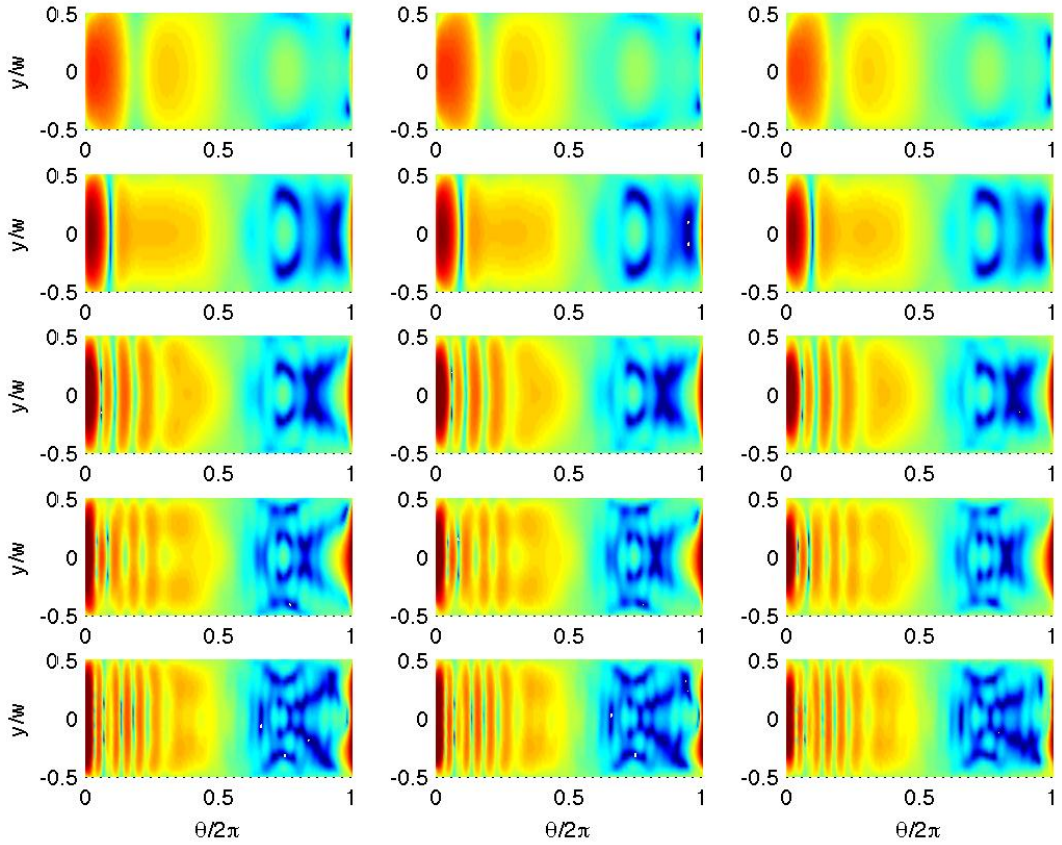

Figure A.4

Horn amplification $20\log_{10}(|H|)$ for the wide tyre geometry (w/R = 1) with: (top to bottom) kR = 3, 6, 9, 12 and 15; (left to right) R_c/R = 0, 0.0625, and 0.125; receiver angle $\phi = 0°$.

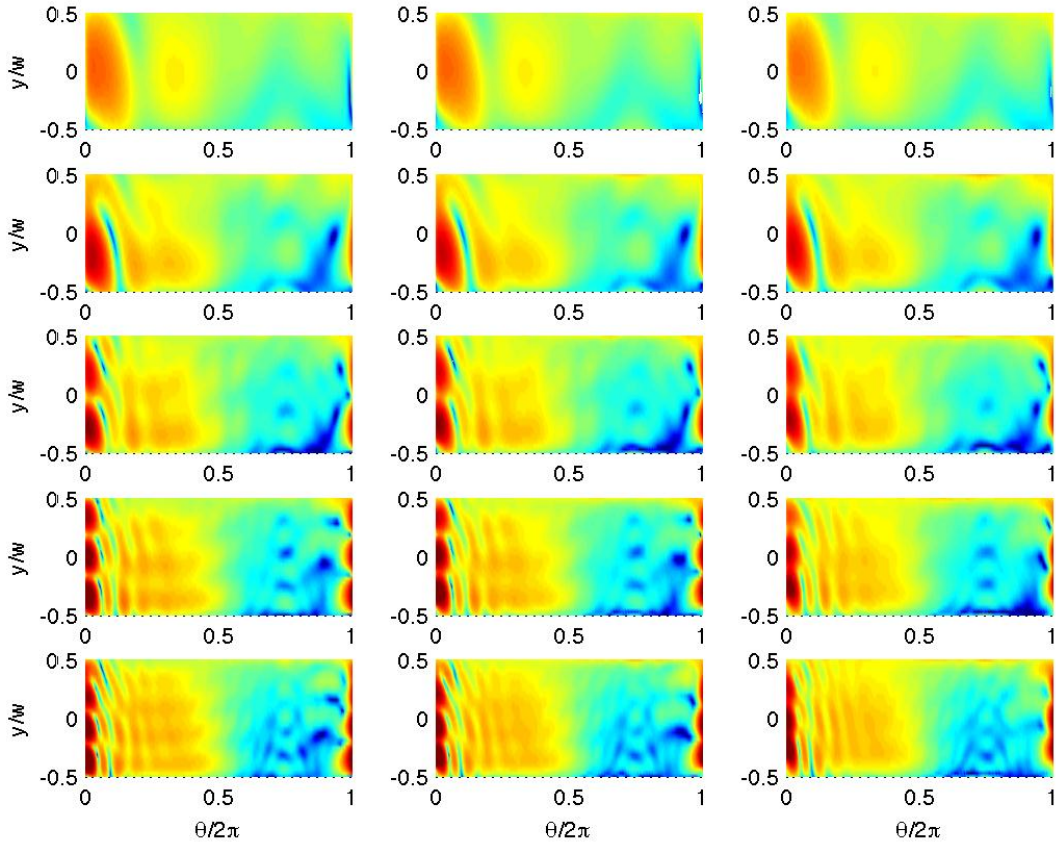

Figure A.5

Horn amplification $20\log_{10}(|H|)$ for the wide tyre geometry (w/R = 1) with: (top to bottom) kR = 3, 6, 9, 12 and 15; (left to right) R_c/R = 0, 0.0625, and 0.125; receiver angle ϕ = 45°.

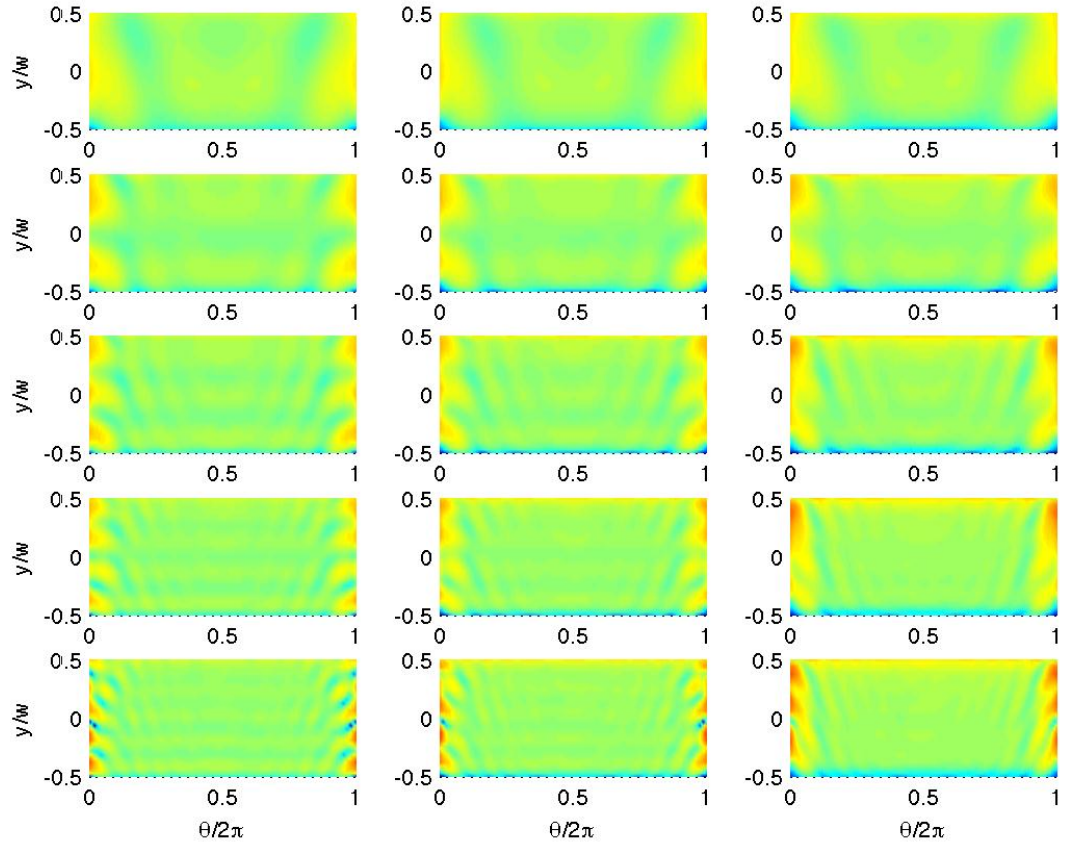

Figure A.6

Horn amplification $20\log_{10}(|H|)$ for the wide tyre geometry (w/R = 1) with: (top to bottom) kR = 3, 6, 9, 12 and 15; (left to right) R_c/R = 0, 0.0625, and 0.125; receiver angle ϕ = 90°.

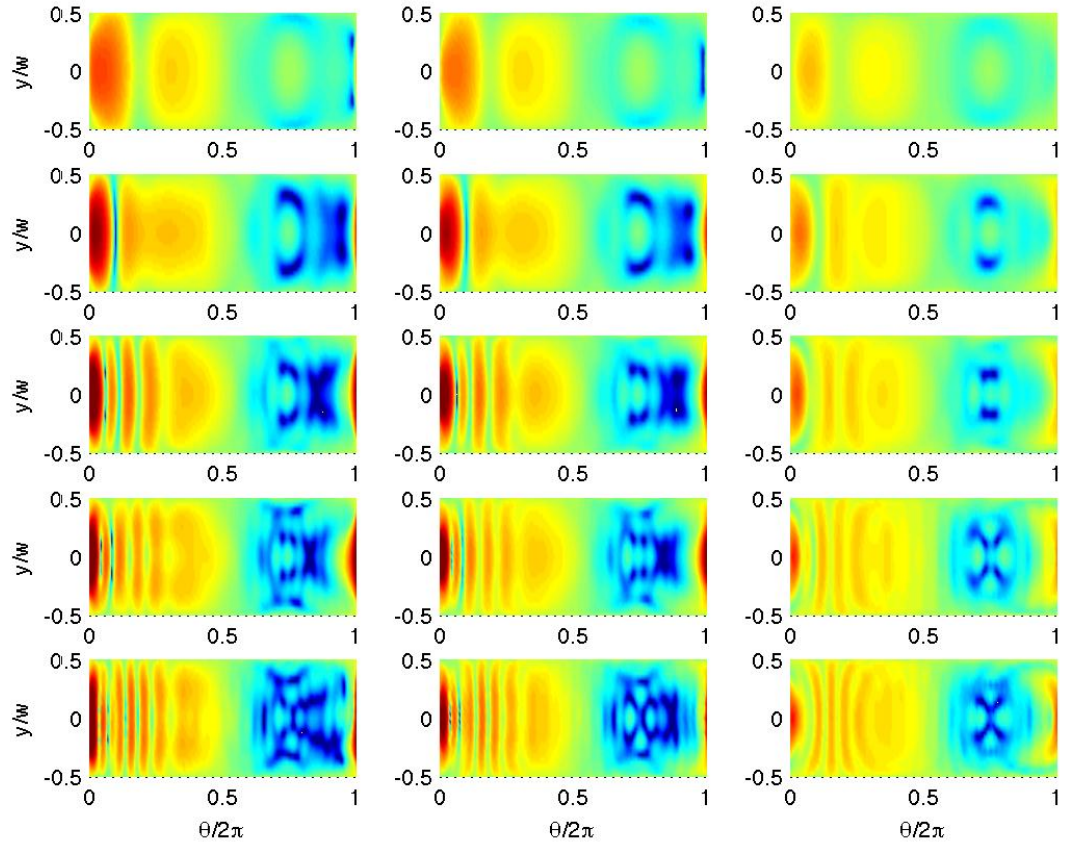

Figure A.7

Horn amplification $20\log_{10}(|H|)$ for the wide tyre geometry (w/R = 1) with: (top to bottom) kR = 3, 6, 9, 12 and 15; (left to right) R_c/R = 0.125, 0.25, and 0.5; receiver angle ϕ = 0°.

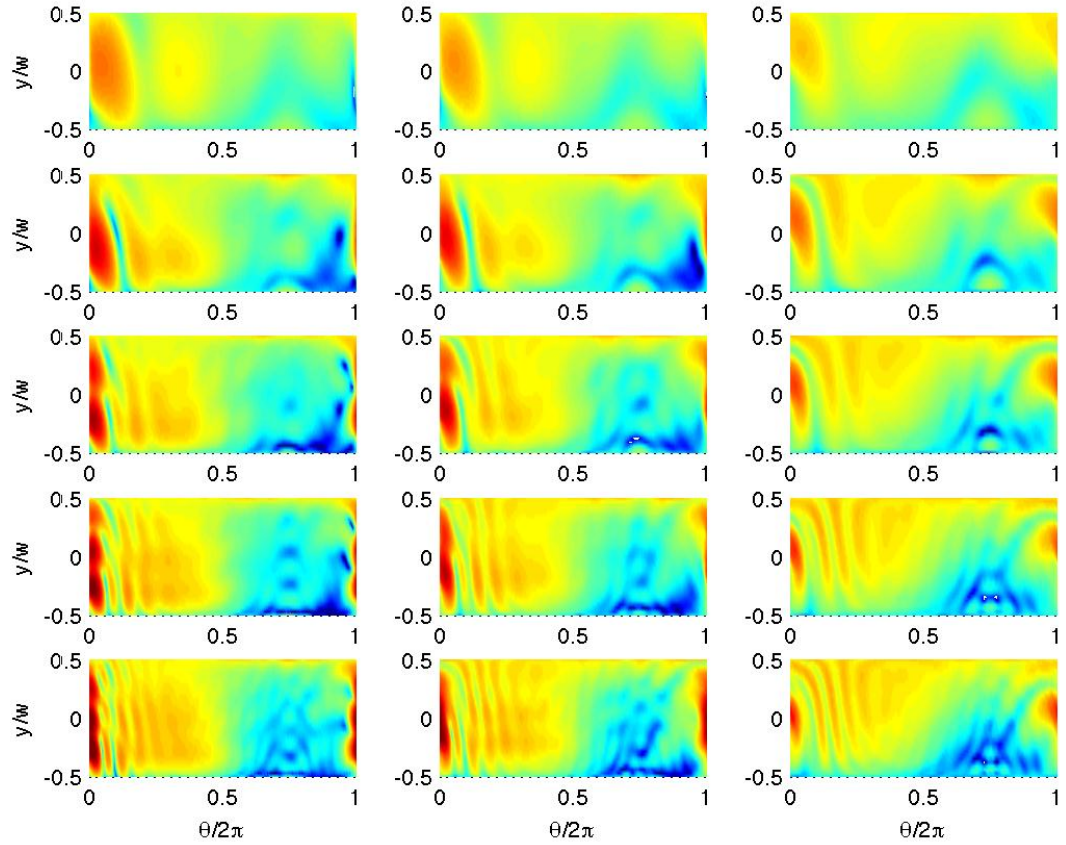

Figure A.8

Horn amplification $20\log_{10}(|H|)$ for the wide tyre geometry (w/R = 1) with: (top to bottom) kR = 3, 6, 9, 12 and 15; (left to right) R_c/R = 0.125, 0.25, and 0.5; receiver angle ϕ = 45°.

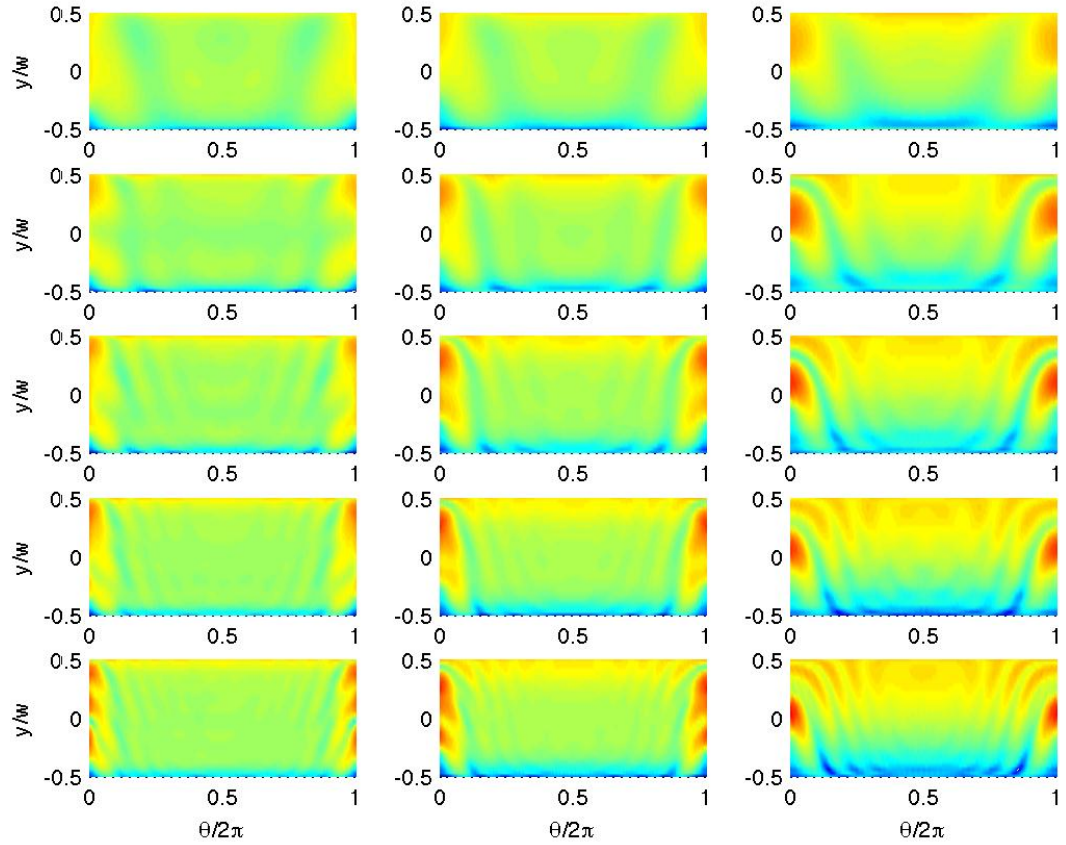

Figure A.9

Horn amplification $20\log_{10}(|H|)$ for the wide tyre geometry (w/R = 1) with: (top to bottom) kR = 3, 6, 9, 12 and 15; (left to right) R_c/R = 0.125, 0.25, and 0.5; receiver angle ϕ = 90°.